June 1999

# Update to the WFPC2 Instrument Handbook for Cycle 9

*To Be Read in Conjunction with the WFPC2 Handbook Version 4.0 Jan 1996*

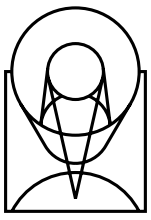

SPACE
TELESCOPE
SCIENCE
INSTITUTE

Science Support Division
3700 San Martin Drive
Baltimore, Maryland 21218
help@stsci.edu

Operated by the Association of Universities for Research in Astronomy, Inc., for the National Aeronautics and Space Administration

## User Support

For prompt answers to questions, please contact the Science Support Division Help Desk.
**E-mail:** help@stsci.edu
**Phone:** (410) 338-1082

## World Wide Web

Information, software tools, and other resources are available on the WFPC2 World Wide Web site:
**URL:** http://www.stsci.edu/instruments/wfpc2

## Revision History

| Instrument | Version | Date | Editor(s) |
|---|---|---|---|
| WF/PC-1 | 1.0; 2.0; 2.1 | October 1985; May 1989; May 1990 | Richard Griffiths |
| WF/PC-1 | 3.0 | April 1992 | John W. MacKenty |
| WFPC2 | 1.0; 2.0; 3.0 | March 1993; May 1994; June 1995 | Christopher J. Burrows |
| WFPC2 | 4.0 | June 1996 | John A. Biretta |
| WFPC2 | Update | June 1998 | Andrew Fruchter, Inge Heyer |
| WFPC2 | Update | June 1999 | Stefano Casertano |

Send comments or corrections to:
Science Support Division
Space Telescope Science Institute
3700 San Martin Drive
Baltimore, Maryland 21218
E-mail: help@stsci.edu

# Table of Contents

CHAPTER 1

# Update to the WFPC2 Instrument Handbook for Cycle 9

**In This Document...**



## Introduction

The Wide Field Planetary Camera 2 (WFPC2) is now a mature and largely well-characterized instrument. Information already available through the *WFPC2 Instrument Handbook* and the *HST Data Handbook* is fairly complete. In this update we provide additional information obtained from recent studies of the instrument, as well as calibration plans for the

WFPC2, and a short note on present and planned imaging capabilities for HST. The major topics discussed in this document are:

- ***Photometric Nonlinearities: Charge Transfer Efficiency and "Long vs. Short" Anomaly:*** Recent tests of the photometric performance of WFPC2 have evidenced significant nonlinearities that can affect its response, especially for very faint sources (< 30 DN of signal per exposure). Measurements of the Charge Transfer Efficiency (CTE) of the WFPC2 charge-coupled devices (CCDs) have shown that the fraction of charge "lost" to impurities in the CCD has grown with time. The CTE loss is particularly high in images with low backgrounds, and can, in some cases, significantly affect photometry. Users who plan to observe in modes that typically produce images with low backgrounds—for instance UV images, narrow-band images, and short exposures—should examine the section on CTE to see how this may affect their program. Another nonlinearity, often referred to as the Long vs. Short anomaly, causes an increasing fraction of the charge to be lost for faint sources, and thus stars appearing slightly fainter in short exposures than in long exposures. Both anomalies have been extensively characterized over the past two years, and approximate correction formulae are now available that should reduce their impact to well below 2% for well-exposed sources, and to about 3% in the worst case (faint sources and low background).
- ***The Stability of the WFPC2 Photometric Calibration:*** The photometric throughput of the clean WFPC2 has remained fairly stable throughout its operational life. However, the rate at which contaminants increase after each decontamination - and thus at which UV throughput is lost - has changed over the years, mostly decreasing due to the cleaner environment of the instrument. We detail the major changes found and indicate for which observations users should consider applying corrections to throughput or contamination rate.
- ***Field and Focus Dependence of Aperture Photometry:*** Small-aperture photometry is sensitive to changes to the WFPC2 Point Spread Function (PSF), which varies as function of filter, focus position, and field position. We give references to correction formulae for both field and focus dependence for the most commonly used filters.
- ***Point-Spread Functions:*** Progress has been made in recent years on the accurate subtraction of WFPC2 PSFs both to detect nearby faint companions of bright stellar objects and to obtain accurate stellar photometry. This document provides a short update describing the imaging dynamic range one can now expect to obtain near a bright stellar source, and our present understanding of the photometric accuracy one can obtain by PSF subtraction.

- ***Dithering:*** Dithering the telescope as a means of improving image resolution and removing detector defects has become increasingly popular among users of WFPC2 since the technique was successfully employed for the Hubble Deep Field. We present some issues related to the use of singly dithered observations (one image at each dither position), and describe how recently developed software can support such observations. The advantage of singly dithered observations is that more dither positions can be obtained in a given amount of time or number of exposures. The disadvantages are that the data are somewhat more difficult to reduce, and stellar photometry to better than a few percent cannot be guaranteed except in cases of excellent dithering coverage. A new document, the Drizzle Cookbook, presents fully worked-out examples of the analysis of dithered data.
- ***Polarization Calibration:*** A comprehensive model developed for the physics of polarization in WFPC2 can be used to derive a more accurate calibration of WFPC2 polarimetric observations, with an estimated accuracy of about 1.5% rms.
- ***Dark Current Change:*** The dark signal seen in WFPC2 images has increased by about 30-120% since launch. Under most circumstances, the dark current remains a modest contribution to the overall image noise. A new superdark has been constructed, based on 1998 data, and is currently in use in the calibration pipeline, thus ensuring correct dark current subtraction.
- ***Operating Changes:*** Some minor changes have been recently introduced in how WFPC2 observations are scheduled. These changes should improve the schedulability of long programs, as well as the overall efficiency of HST observations.
- ***Other Instruments:*** In addition to WFPC2, HST currently has another operating instrument capable of imaging, the Space Telescope Imaging Spectrograph (STIS). STIS may be preferable to WFPC2 for some imaging programs. A new instrument, the Advanced Camera for Surveys (ACS), will be installed on HST in 2000, and will be offered for observations during Cycle 10. We provide a short overview of the current and planned capabilities of these instruments, comparing them with WFPC2.
- ***WFPC2 Clearinghouse:*** The WFPC2 group has developed a web-based tool, the WFPC2 Clearinghouse, to allow users to easily search journal articles, STScI documentation, and user-submitted documents for topics relating to the performance, calibration, and scientific use of WFPC2. This tool is described in the hope that the information made available by its use will help observers in the preparation of their observing plans, as well as in the reduction of their data.

- ***Calibration Plans:*** Calibration of WFPC2 continues. We provide an updated table of system efficiencies and zeropoints, which differs slightly from that in the Instrument Handbook for certain narrow-band and UV filters. We also describe the plans for future calibration of WFPC2. Users who suspect that they will have unusual or particular calibration needs should examine the calibration plan to determine if they will need to take their own calibration observations as part of their HST observing program.

# Photometric Anomalies

***To be read in conjunction with Chapter 6 of the*** *WFPC2 Instrument Handbook,* ***Version 4.0.***

Two photometric anomalies resulting from nonlinearities of the WFPC2 detectors have now been extensively characterized. The first is due to the imperfect charge transfer efficiency (CTE) of the detectors, which causes sources at high row and column numbers to appear fainter because the charge is transferred over a bigger fraction of the chip. This anomaly is increasing with time, especially for faint sources, presumably as a consequence of on-orbit radiation damage. The second, called “long vs. short”, causes sources to have a lower count rate - and thus appear fainter - in short exposures than in longer exposures, and appears independent of the position on the chip. The physical cause of the long vs. short anomaly is not fully understood, and it does not appear to change with time. We have developed correction formulae which appear to reduce the impact of both anomalies to about 2-3% for faint sources.

## Charge Transfer Efficiency

During the past two years, two studies were completed resulting in a better characterization of the Charge Transfer Efficiency (CTE) problem for WFPC2, based on an analysis of observations of the globular cluster ω Cen (NGC 5139). The first study provides a set of formulae that can be used to correct for CTE loss when doing aperture photometry, based on a dataset taken on June 29, 1996 (Whitmore and Heyer 1997).[1] The second study found evidence that CTE loss for faint stars has increased with time (Whitmore, 1998). A third study (Whitmore, Heyer and Casertano 1999) is

1. Please refer to the list of “References” on page 45.

currently being prepared for publication, and will supersede the earlier work. Please check our web pages for updated information.

Figure 1.1: Ratio of count rates observed for the same star (i.e., throughput ratio) as a function of the change in row position for stars in 4 different brightness ranges. The negative slope shows that a star appears brighter when it is at low row number, thus closer to the “bottom” of the chip and the readout amplifiers, than when it is at high row number. The effect is larger for fainter stars. See Whitmore and Heyer (1997) for details.

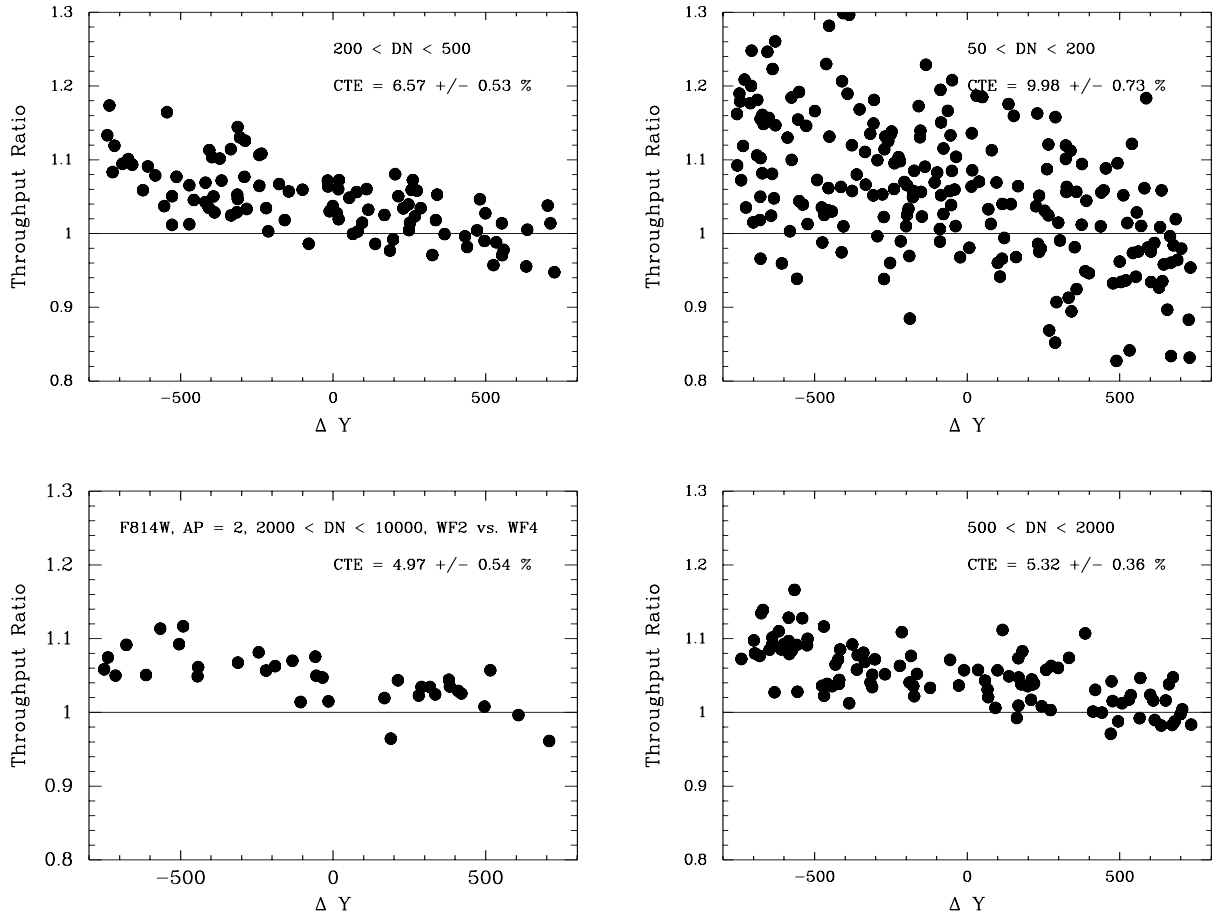


The primary observational consequence of CTE loss is that a point source at the top of the chip appears to be fainter than if observed at the bottom of the chip, due to the loss of electrons as the star is read out down the chip (see Figure 1.1). This is called *Y-CTE*. There also appears to be a similar, but weaker tendency, for stars on the right side of the chip to be fainter (called *X-CTE*). The effects also depend on the brightness of the star and the background level. Formulae are presented in WFPC2 ISR 97-08 that reduce the observational scatter in this particular dataset from 4–7% to 2–3%, depending on the filter.

Figure 1.2: Y-CTE loss as a function of time for different target brightness (Whitmore et al 1999). Different symbols correspond to different background levels. The straight lines represent the best-fit multilinear regression for Y-CTE as function of time, log counts and log background, as discussed in Whitmore et al (1999).

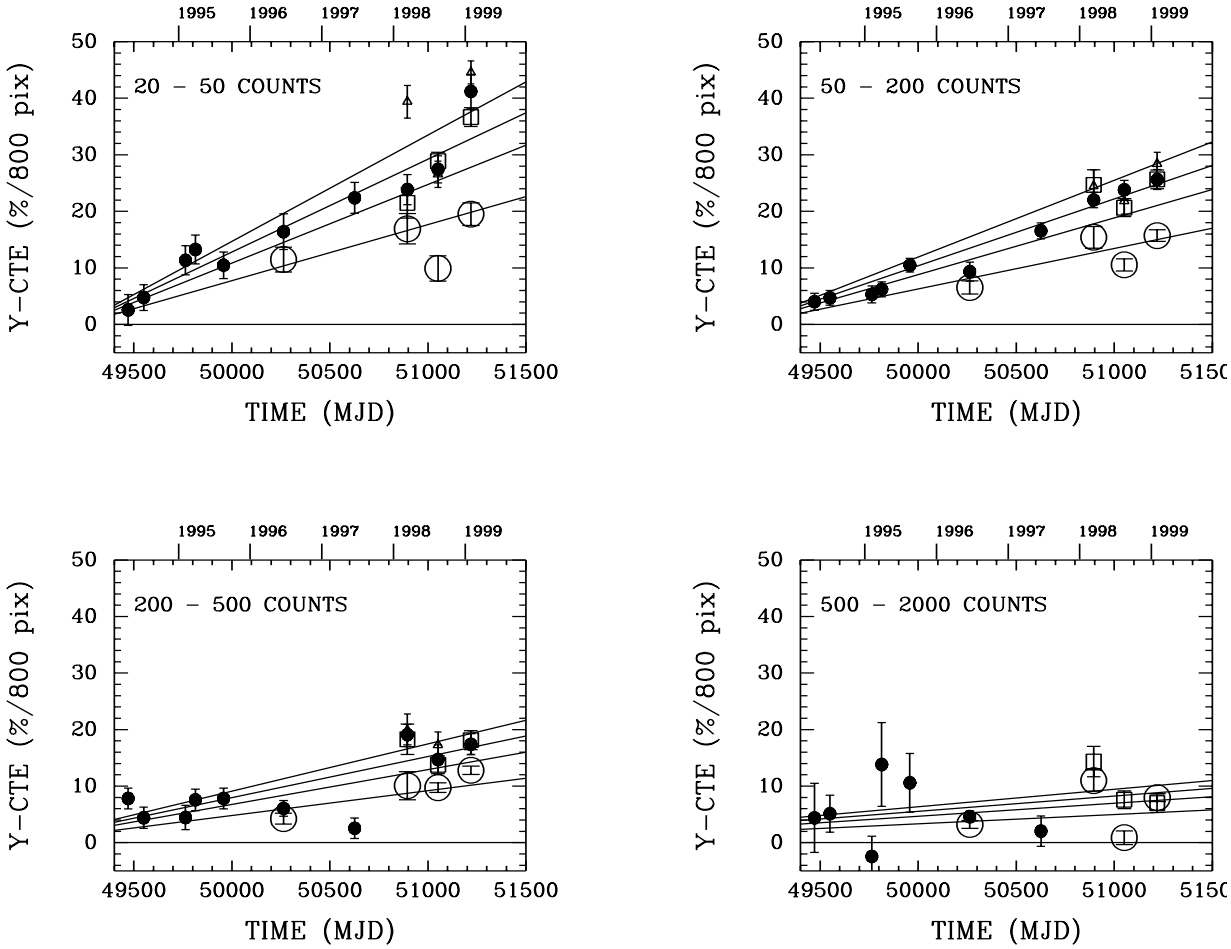


A continuation of this analysis using new observations of ω Cen suggests that the CTE loss for WFPC2 is time dependent. The datasets cover the time range from April 28, 1994 (shortly after the cooldown) to February 1999. For bright stars (i.e., brighter than 200 DN when using gain = 15; equivalent to 400 DN for gain = 7) there is only a modest increase in the amount of CTE loss as a function of time. However, for faint stars the CTE loss has increased more rapidly. For example, for very faint stars (i.e., 20–50 DN at a gain of 15) the CTE loss has increased from 3% to 40% for a star at the top of the chip. There is no obvious change in the value of X-CTE

It should be noted that these results are based on very short (14 second) exposures, with a very low background level (the observations used in Figure 1.2 have a typical background of ~0.1 DN/pixel). Typical WFPC2 exposures are much longer than these short calibration images, resulting in

higher background levels, which significantly reduce the CTE loss and minimize the CTE problem for most science observations.

Observers can use a number of strategies to minimize the effect of CTE loss. Longer individual exposures help by increasing both background and source counts, both of which reduce CTE loss. Users thinking of dithering may wish to take this into account if they are considering shortened exposures to allow for more dither positions. When observing a target significantly smaller than a single detector, it is advisable to place it towards the bottom of a chip; the aperture WFALL will place the target near the bottom of Chip 3. (Note however that targets larger than about 20" centered on WFALL will be split between chips, with a possible impact on photometric accuracy.) The resulting photometry can be corrected after the fact using the formulae provided in the references above; however, when the highest possible accuracy is required, another possibility is to include a special calibration observation of ω Cen, taken close to the time of the science observations and designed so as to reproduce them as closely as possible in exposure and background levels.

A further possible strategy is to preflash the chip to raise the background. However, tests indicate that the required level of preflash is so high that in general more is lost than gained by this method. A variation of this is currently being tested in the “noiseless” preflash proposal (8450), where a flatfield exposure is read out immediately prior to a short science exposure.[2]

As part of the Cycle 8 Calibration Plan, in addition to the noiseless preflash test, we will continue monitoring the CTE for point sources by repeating the key observations of ω Cen every six months (Proposal 8447). We have also added observations of a cluster of galaxies (Proposal 8456), which will yield a direct measurement of the effect of CTE for faint extended sources for more typical exposure times and background levels.

## The Long vs. Short Photometric Anomaly

The so-called “long vs. short” anomaly is a nonlinearity of WFPC2 which causes the recorded count rate to increase with exposure time for a given source - the source thus appears brighter in a long exposure than in a short exposure. A recently completed study of this anomaly (Casertano and Mutchler 1998) shows that it is primarily a function of the total source counts, and, unlike the CTE anomaly, is independent of the position in the chip. In the simplest interpretation, a fraction of the total counts are lost, with the fraction decreasing as the source counts increase. The fraction lost is about 3% for a source with 300 counts, and rises to over 20% at 40 counts. Sources over 1000 counts are not measurably affected. There

2. More details can be found in Biretta and Mutchler (1998) and Whitmore (1998).

appears to be a weak dependence on background, in the sense that the loss of signal is slightly lower in high-background images, but this effect is not significant in terms of the overall characterization of the correction.

Figure 1.3: Magnitude discrepancy for exposure times from 10s to 1000s in F814W, plotted against total measured counts. Some exposures have been pre-flashed with 5 to 1000 e/pixel. The major trend is against total counts.

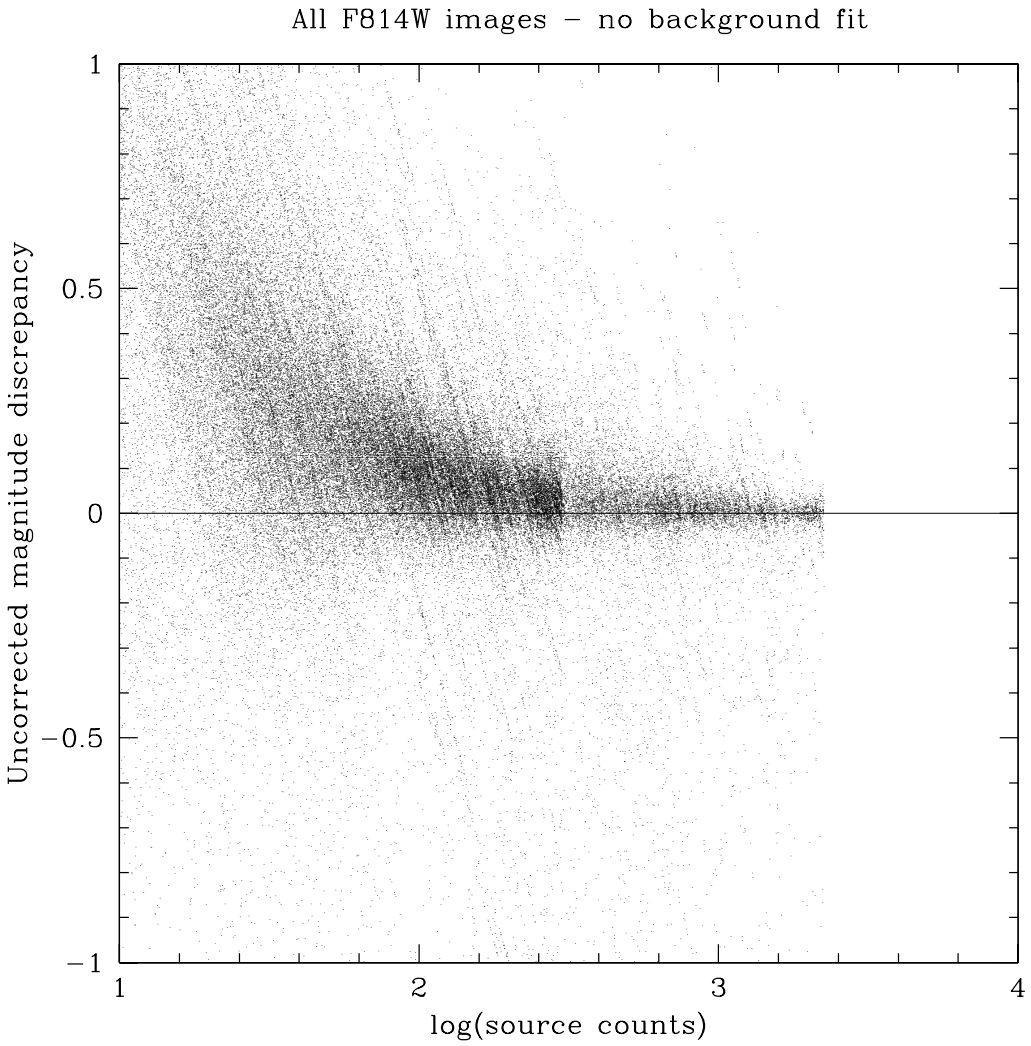


We have developed a simple correction formula that can be used to compensate approximately for the signal lost. The formula expresses the magnitude correction *dm* to be subtracted from the measured magnitude:

$$dm = \frac{0.629}{1 + 0.0315 \cdot counts + 0.000333 \cdot counts^2} \qquad (1)$$

as a function of *counts*, the background-subtracted source counts in a 2-pixel aperture, measured in DN at gain 7. Note that the correction formula is applied *after* the CTE correction discussed in the previous Section has been made.

Figure 1.3 shows the uncorrected magnitude errors for individual F814W observations of a field in NGC 2419 containing stars of various magnitudes, observed with exposure times ranging from 10s to 1000s and various preflash levels. The anomaly is illustrated by the rise in magnitude errors for low source counts. The effect of our correction is shown in Figure 1.4, where the solid line and error bars plot the median and quartiles of uncorrected magnitude errors, while the dashed line indicates the median of the residual magnitude errors, after the correction in Equation (1) is applied. Magnitude errors are corrected quite well, except for very faint sources (< 30 counts).

Figure 1.4: Median and quartiles of the magnitude discrepancy, before and after the correction in Equation (1) has been applied (solid and dashed lines, respectively).

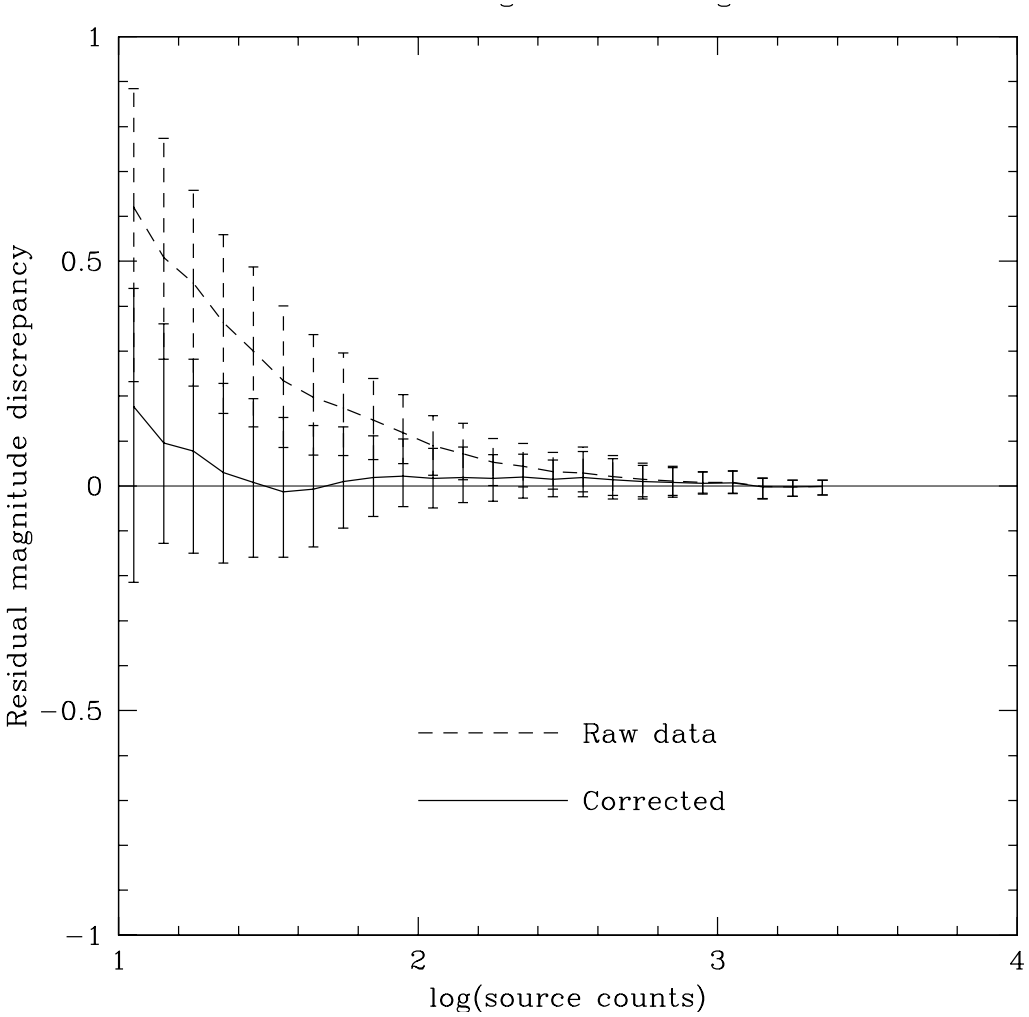

On the basis of the evidence collected so far, the anomaly appears to be more properly a function of total counts in a stellar image, rather than a direct function of exposure time. The commonly used “long vs. short” name is thus somewhat of a misnomer.

It should be emphasized that the correction in Equation (1) has been derived from a specific set of conditions, and may not be valid in general. Specifically, images obtained by combining several subexposures and images taken at gain 15 have not been studied. Casertano and Mutchler (1998) provide some suggestions on how to handle such cases. Further data, including a test of the noiseless preflash, will be taken as part of the Cycle 8 calibration program.

# The Stability of WFPC2 Photometric Calibration

***To be read in conjunction with Chapter 6 of the*** *WFPC2 Instrument Handbook,* ***Version 4.0.***

The long-term photometric stability of WFPC2 has been evaluated by examining the photometric monitoring data collected over a period of more than four years. Our primary standard, GRW+70D5824, has been observed roughly every four weeks, before and after decontamination procedures, both in the far UV and in the standard photometric filters. Early observations were taken monthly in both the PC and WF3; since Cycle 6, we have switched to a rotation schedule, where observations are taken in a different chip each month. Overall, a baseline of over four years is available for the PC and WF3, and about two and a half years in WF2 and WF4. The data have been analyzed and reported by Baggett and Gonzaga (1998); here we summarize their main conclusions.

Overall, the WFPC2 photometric throughput, as measured via our primary standard, has remained remarkably stable throughout. Its long-term behavior in filters longward of F336W is characterized by small fluctuations (2% peak-to-peak) which appear to have no specific pattern, and there is no significant overall sensitivity trend. Aside from contamination corrections, which are only significant shortward of F555W, the same photometric zeropoints can be applied to non-UV data throughout the life of WFPC2.

In contrast, the UV photometric throughput of WFPC2 has changed measurably over the years. In most cases, the throughput has increased slowly, perhaps as a result of continuing evaporation of low-level contaminants; in F170W, the best-characterized UV filter on WFPC2, the clean throughput (immediately after a decontamination) has increased in

the PC by about 9% since 1994. This behavior is not uniform, in that some UV filter/detector combinations show a modest decline in throughput (3% in F255W). Baggett and Gonzaga (1998) report the details of the secular throughput changes for the filters we monitor.

Finally, the contamination rates - the rate at which the camera throughput declines after a decontamination, due to the gradual buildup of contaminants on the cold CCD windows - have generally decreased since installation of WFPC2, possibly also because the environment has become cleaner with time. (This excludes a brief period of increased contamination just after the second servicing mission.) For example, the contamination rate in F170W in the PC has decreased from 0.56%/day to 0.45%/day.

Baggett and Gonzaga (1998) suggest a number of ways users can correct long-term changes in WFPC2 photometry. While these changes are generally small, users wishing to achieve high-precision photometry, especially in the UV, should follow their recommendations.

# Field and Focus Dependence of Aperture Photometry

***To be read in conjunction with Sections 5.4-5.7 of the*** *WFPC2 Instrument Handbook,* ***Version 4.0.***

Photometry of point sources in WFPC2 data is most often accomplished via aperture photometry using a fairly small aperture radius (2 to 5 pixels). An aperture correction is then needed to estimate the counts outside the aperture, which often cannot be measured directly because of noise, background fluctuations, or crowding. Since the WFPC2 PSF is a function of focus, filter, and position within the field of view, the aperture correction will also change with these parameters. The changes are most significant for small apertures (< 2 pixel radius), and become negligible at apertures larger than 5 pixels.

Two studies have sought to characterize the change in aperture correction under various conditions. Suchkov and Casertano (1997) discuss the variation in WFPC2 focus and its impact on the aperture correction The HST focus varies due to a combination of circumstances: long-term shrinkage of the metering truss that supports the HST secondary, compensatory moves made at approximately six-month intervals to compensate for this shrinkage, and temperature fluctuations in HST, which produce variations on time scales of hours to months. For more information, see the HST focus web site at

http://www.stsci.edu/instruments/observatory/focus/focus2.html.

Suchkov and Casertano (1997) find that the aperture correction varies with focus by up to 10% for a 1-pixel radius in the PC, and is generally well-fitted by a quadratic function of focus position. A 10% change is measured only for 5 micron defocus, which is the largest that can be expected during normal telescope operations. The variation in aperture correction is much smaller in the WF cameras and for apertures of 2 pixels or larger, which are less sensitive to the small HST defocus. Formulae that estimate the change in aperture correction due to defocus are provided for a variety of circumstances.

More recently, Gonzaga et al. (1999) have characterized the change in aperture correction as a function of filter and field position. The data are somewhat incomplete, but a clear trend is present: the aperture correction generally increases linearly as a function of distance to the chip center (see Figure 1.5). For example, the aperture correction from 1 to 5 pixel radius in the PC increases by about 0.12 mag from the chip center to the edge.

Figure 1.5: Measured aperture corrections for different stars observed in the PC through filter F555W. The dominant term appears to be linear with the distance R to the chip center.

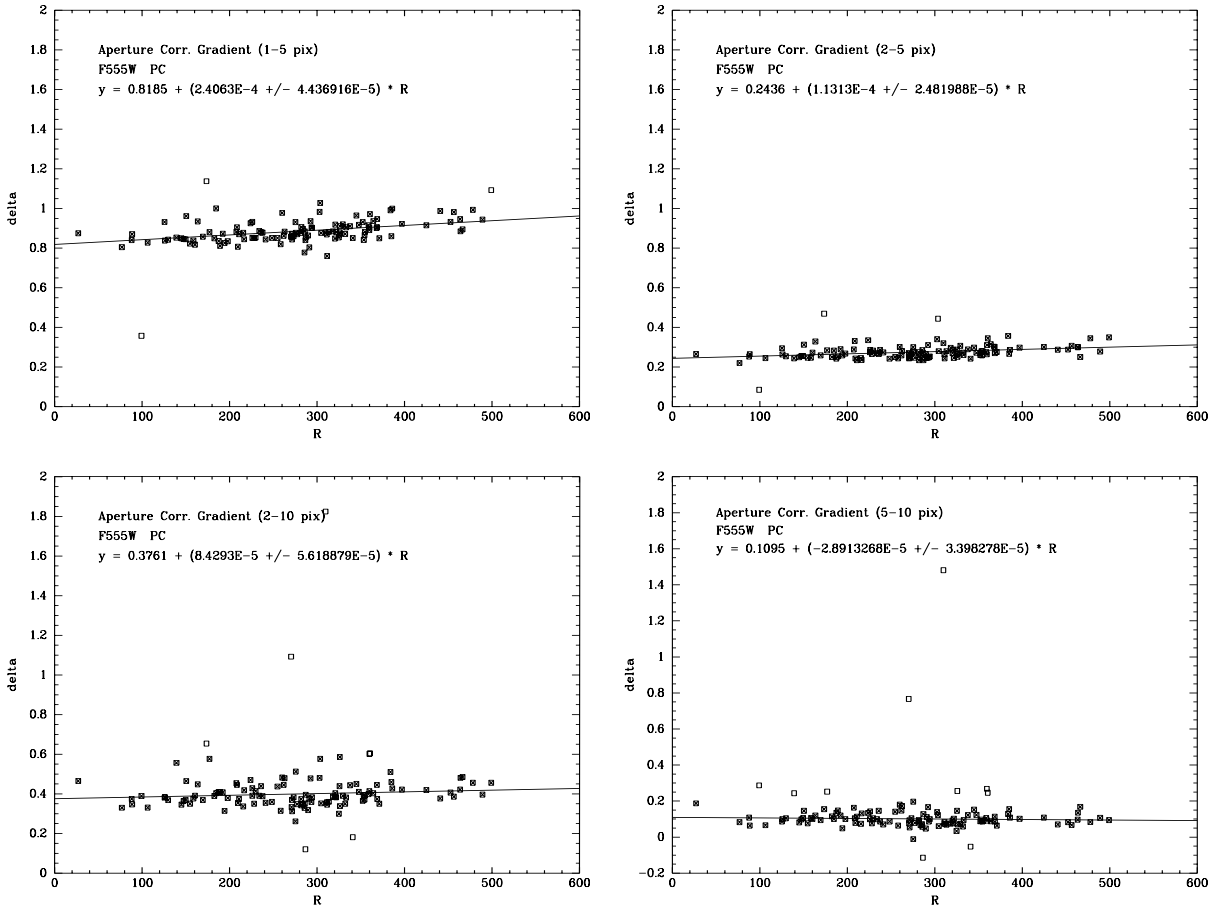

In practice, the interplay between aperture correction and defocus may be complex, since the optimal focus changes with focus and field position. A full correction has not been established, but the TinyTim PSF model (see next Section) can be used to estimate the extent of the variation in aperture correction. In general, we recommend that a minimum aperture radius of 2 pixels be used whenever possible, in order to minimize the impact of variations of the aperture correction with focus and field position; if the field is too crowded for this strategy to be used, we recommend that users verify the validity of the corrections given on a few well-exposed stars.

# The WFPC2 PSF: Dynamic Range and Photometry

***To be read in conjunction with Chapter 5 of the*** *WFPC2 Instrument Handbook,* ***Version 4.0.***

Here we supplement the Instrument Handbook with short discussions of the use of PSF subtraction to maximize image dynamic range and to obtain accurate stellar photometry. We also discuss a source of error in the published values of the HST aperture corrections.

## Dynamic Range

The WFPC2 PSF has structure on very small scales, with significant power on scales smaller than 1 PC pixel. Thus faint objects near bright objects can be difficult to detect and to distinguish from PSF artifacts. Model PSFs (for example those produced by the TinyTim software[3]) are quite good for many purposes, but can leave residuals as large as 10 to 20% of the peak.

Recent results indicate that PSF subtraction and detection of faint objects very close to bright objects can be improved by using a composite PSF from real data, especially dithered data. Table 1.1 on page 14 indicates limits that may be obtained for well-exposed sources (nominal S/N > 10 for the faint object) where a dithered PSF image has been obtained.

A technique that has been used with some success to search for nearby neighbors of bright stars is to image the source at two different roll angles, and use one observation as the model PSF for the other. In the difference image, the secondary source will appear as a positive residual at one position and a negative residual at a position separated by the change in roll

3. http://scivax.stsci.edu/~krist/tinytim.html

angles. PSF artifacts generally do not depend on roll angle, but rather are fixed with respect to the telescope. Thus, small changes in the PSF between observations will not display the positive or negative signature of a true astrophysical object. Again, it is recommended that the observations at each roll angle be dithered.

Table 1.1: Limiting Magnitudes for PSF Subtraction Near Bright Objects

| Separation in arcsec (on PC) | Limiting Δm (without PSF subtraction) | Limiting Δm (with PSF subtraction) |
|---|---|---|
| 0.15 | 2.5 | 5.0 |
| 0.25 | 4.5 | 6.4 |
| 0.4 | 6.5 | 7.3 |
| 1.0 | 8.9 | 10.7 |
| 3.0 | 10.7 | 12.9 |

## Photometry

PSF subtraction is also an effective means of accurate and repeatable photometry on HST. Papers presented at the 1997 HST Calibration Workshop by Remy et al. and Surdej et al. show that the subtraction of synthetic or scaled observed PSFs can be used to obtain 1–2% stellar photometry.

In spite of the ability to obtain photometry through PSF subtraction, the total fraction of the light of the PSF within a given radius is not known to better than a few percent due to the difficulty of measuring the light in the faint wings of stellar PSFs (remember that there are over 17,000 PC pixels inside a radius of 3″, each contributing read noise to the observation!). This difficulty has contributed to a minor error in Table 6.7 of the *WFPC2 Instrument Handbook*, which gives the fraction of encircled energy in the F555W filter within a 1″ radius as 100%. This table is based upon the encircled energy figures from Table 2(a) of Holtzman et al. (1995a). Examination of several filters shows that about 10% of the light in the PSF is missing at 1″ in the PC. Observers estimating aperture corrections for their images should be wary of this effect and note that in a later paper (Holtzman et al. 1995b) the same group normalized the HST magnitude system to the light enclosed inside of a 0.″5 radius to minimize errors caused by the uncertain aperture correction at large radii.

# Dithering with WFPC2

***To be read in conjunction with Section 7.6 of the** WFPC2 Instrument Handbook**, Version 4.0***

Dithering is the technique of displacing the telescope between observations either on integral pixel scales (to assist in removing chip blemishes such as hot pixels) or on sub-pixel scales (to improve sampling and thus produce a higher-quality final image). The *WFPC2 Instrument Handbook* provides a good introduction to dithering strategies in Section 7.6; however, our experience with processing dithered WFPC2 data has progressed substantially over the last two years, and new software tools have been introduced which make the combination of dithered data both easier and more efficient. The method we recommend is based on the "variable pixel linear reconstruction" algorithm, also known as "drizzle" (Fruchter and Hook 1997). This method has been developed into a number of tasks, incorporated into the IRAF/STSDAS packages **dither** and **ditherII**, which allow effective cosmic ray removal from singly dithered data (i.e., only one image per pointing). The **dither** package is part of the standard STSDAS distribution, while the **ditherII** package is available for download via the web at:

http://www.stsci.edu/~fruchter/dither/#DitherII.

We anticipate that **ditherII** will be incorporated into the standard STSDAS distribution during 1999. With this software, it is now practical to obtain high-quality images via dithering even when the available time does not permit obtaining a CR-split at each pointing, and dithering is recommended under most circumstances (subject to the cautions further below).

Further information on the software in development to process dithered data can be found in two papers in the *1997 HST Calibration Workshop Proceedings*: "A Package for the Reduction of Dithered Undersampled Images," by Fruchter et al. (1997), and "Dithered WFPC2 Images—A Demonstration," by Mutchler and Fruchter (1997). Up-to-date information about dithering and related issues can also be found on the WFPC2 drizzling web site at:

http://www.stsci.edu/instruments/wfpc2/Wfpc2_driz/wfpc2_driz.html

In order to help users reduce dithered images, we have prepared the *Drizzling Cookbook* (Gonzaga et al 1998), also available at the URL above. This document gives a general outline of the reduction of dithered images and provides step-by-step instructions for six real-life examples that cover a range of characteristics users might encounter in their observations. The

data and scripts needed to reproduce the examples are also available via the same URL.

Despite all the improvements in the combination of dithered images, users should be mindful of the following cautionary notes:

- Processing singly dithered images can require substantially more work (and more CPU cycles) than processing data with a number of images per pointing.
- Removing cosmic rays from singly dithered WFPC2 data requires good sub-pixel sampling; therefore one should probably not consider attempting this method with WFPC2 using fewer than four images and preferably no fewer than six to eight if the exposures are longer than a few minutes and thus subject to significant cosmic ray flux.
- It is particularly difficult to correct stellar images for cosmic rays, due to the undersampling of the WFPC2 (particularly in the WF images). Therefore, in cases where stellar photometry to better than a few percent is required, the user should take CR-split images, or be prepared to use the combined image only to find sources, and then extract the photometry from the individual images, rejecting entire stars where cosmic ray contamination has occurred.

Figure 1.6: On the left, a single 2400s F814W WF2 image taken from the HST archive. On the right, the drizzled combination of twelve such images, each taken at a different dither position.

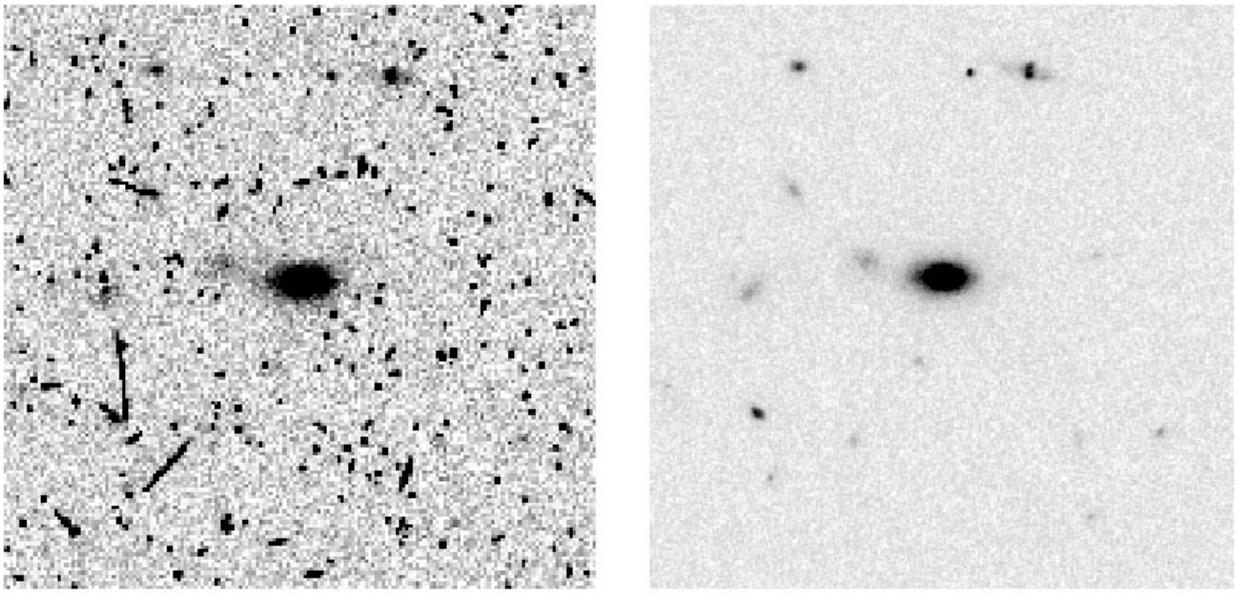

- Offsets between dithered images must be determined accurately. The jitter files, which contain guiding information, cannot always be relied upon to provide accurate shifts. Therefore, the images should

be deep enough for the offsets to be measured directly from the images themselves (typically via cross-correlation). In many cases, the observer would be wise to consider taking at least two images per dither position to allow a first-pass removal of cosmic rays for position determination.

- Finally, and perhaps most importantly, dithering will provide little additional spatial information unless the objects under investigation will have a signal-to-noise per pixel of at least a few at each dither position. In cases where the signal-to-noise of the image will be low, one need only dither enough to remove detector defects.

# Other HST Imaging

***To be read in conjunction with Section 1.2 of the*** *WFPC2 Instrument Handbook,* ***Version 4.0***

The Space Telescope Imaging Spectrograph (STIS) offers imaging capabilities in both the optical and ultraviolet that for some limited applications provides performance superior to that of WFPC2. The interested reader should refer to the Cycle 9 Call for Proposals for a brief overview, and the updated *STIS Instrument Handbook*, version 3, May 1999 and Section 1.2 of the *WFPC2 Instrument Handbook*, version 4, for more details.

Associated with this Cycle 9 Call for Proposals is a preview of the Advanced Camera for Surveys, which will be available for General Observer proposers in Cycle 10. Observers may wish to take into account the future enhancement in HST imaging capabilities promised by the Advanced Camera in order to develop a long term proposal strategy.

# Polarization Calibration

***To be read in conjunction with Section 3.5 of the*** *WFPC2 Instrument Handbook,* ***Version 4.0.***

New calibration observations have permitted a substantial improvement in the polarization calibration of WFPC2 since Cycle 6. The new results, fully described in Biretta and McMaster (1997), are based on a physical

model of the polarization effects in WFPC2, described via Mueller matrices, which includes corrections for the instrumental polarization (diattenuation and phase retardance) of the pick-off mirror, as well as the high cross-polarization transmission of the polarizer filter. New polarization flatfields are also available. Comparison of the model against on-orbit observations of polarization calibrators shows it predicts relative counts in the different polarizer/aperture settings to 1.5% RMS accuracy.

To assist in the analysis of polarization observations, we provide two Web-based utilities, available at

http://www.stsci.edu/instruments/wfpc2/wfpc2_pol_top.html

by which users can simulate and calibrate their data. These tools have been upgraded to include effects related to the $MgF_2$ coating on the pick-off mirror, as well as the more accurate matrices for the cross-polarization leakage in the polarizer filter. Differences between the previous and current versions of the tools are typically around 1% in fractional polarization.

# Dark Current Increase

***To be read in conjunction with Section 4.8 of the*** *WFPC2 Instrument Handbook,* ***Version 4.0.***

Recent measurements of the dark current in the WFPC2 detectors indicate that the average level of dark current has been slowly increasing over the instrument's lifetime. Baggett et al (1998) have re-analyzed dark current measurements taken at regular intervals from 1994 to 1998. Over this five-year period, the dark current has increased by a factor of about 2.2 in the WFC CCDs and by a factor of 1.3 in the PC (values are for the center of the CCDs). A small increase in the cold junction temperatures over this time period was detected as well; however, the amount of temperature change accounts for only a very small portion of the increase in dark current. The dark current increase is smaller in the optically vignetted regions near the CCD edges, suggesting that some of the effect may be caused by increased fluorescence or scintillation in the CCD windows, rather than by the CCDs themselves.

Note that the increase in dark signal we report here affects all pixels, and thus is distinct from the cyclic increase in the number of hot pixels reported in the WFPC2 Handbook. The latter are highly localized, and are almost certainly due to radiation-damaged sites on the CCD detectors. Since the dark current is generally a minor contributor to the total noise in WFPC2 images, its increase is unlikely to impact adversely the quality of WFPC2 observations, except perhaps in special cases (faint sources observed in

AREA mode through narrow-band or UV filters). A new superdark has been generated from 120 dark frames taken around mid-1998 and is currently in use in the calibration pipeline; this superdark provides dark current subtraction consistent with our most recent measurements, and will be updated as needed.

# Operating Changes

Some changes in WFPC2 operations have recently been introduced, primarily in order to increase the scheduling efficiency of HST observations in Cycle 8.

First, the South Atlantic Anomaly (SAA) contours used to limit WFPC2 observations have been modified slightly. The SAA is a region where irregularities in the Earth's magnetic field cause very high cosmic ray rates. WFPC2 imaging is generally not scheduled near the SAA, so as to avoid excessive cosmic ray hits which degrade images by obliterating data in numerous pixels. These adverse effects are usually minimized by operating each instrument only when HST is outside a designated "SAA avoidance contour," although WFPC2 observations of time-critical phenomena can be taken inside the SAA avoidance contour. Biretta and Baggett (1998) have analyzed available WFPC2 data, together with data from Air Force satellites flying in similar orbits, and have redefined the WFPC2 SAA avoidance contour. This change results in a 3% increase in designated SAA-free orbits, which allows better scheduling efficiency, and is expected to impact negatively less than 0.1% of WFPC2 science observations.

Second, WFPC2 visits are now limited to a maximum length of 5 orbits. Very long visits (up to the previous maximum of 8 orbits) have very limited opportunities for scheduling, reduce the efficiency of telescope use, and can cause long delays in execution, with long GO wait times. The transition to shorter visits improves the scheduling opportunities for large proposals. One possible drawback is the lower pointing repeatability across visits; this is likely to be significant only for programs with special dithering requirements.

A third change for Cycle 8 is that an extra minute of overhead has been added to each orbit in RPS2, which allows splitting an orbit in the phase 2 proposal into two separate spacecraft alignments. This one-minute "efficiency adjustment" allows much more efficient scheduling of HST orbits impacted by the SAA.

# The WFPC2 Clearinghouse

The WFPC2 Clearinghouse is a web-based tool designed to provide users with a searchable listing of all known journal articles, STScI documentation and reports, as well as user-submitted documents which report on all aspects of the performance, calibration, and scientific use of WFPC2. The Clearinghouse can be found at:

http://www.stsci.edu/instruments/wfpc2/Wfpc2_clear/wfpc2_clrhs.html

The primary goal of the Clearinghouse is to make it easier for WFPC2 users to take advantage of the fact that there are hundreds of researchers reducing and analyzing WFPC2 data, and of their results.

We have extensively searched through the astronomical literature and selected all articles that contain any reference or description of the calibration, reduction, and scientific analysis of WFPC2 data prior to 1998. Each article was then added to our database, with an estimate of its importance in up to 50 calibration topics. Each entry has the following format:

```
Author: Holtzman,Mould,Gallagher, et al.
Title: Stellar Populations in the Large Magellanic Cloud:
Evidence for..
Year: 1997
Reference: AJ 113, 656
Science Keyword: IMF,LMC
Calibration Keyword(3): psf_fitting_photometry(3)
Calibration Keyword(2): bias(2)
Calibration Keyword(1): photometric_zeropoint(1)
Comment: Comparison of aperture and PSF fitting photometry,
```

where the category number following each keyword stands for the following:

- (3)= One of the fundamental references on this topic.
- (2)= Some new information on this topic.
- (1)= General information on the subject.

The user can select from a large list of WFPC2 calibration related topics (see below). The results from a Clearinghouse search will list, alphabetically by author, all articles containing references to the selected topic. For journal articles, each reference is linked to that article's entry in the ADS Abstract Database, so that users can quickly determine if that particular article is relevant to their individual needs.

The following topics are available:

| | |
|---|---|
| Aperture Corrections | Object Identification |
| Aperture Photometry | Observation Planning |
| Astrometry | Photometric Transformations |
| Bias Frames | Photometric Zeropoint |
| Bias Jumps | Pipeline Calibration |
| Calibration Observations | Polarization |
| CCD Characteristics | PSF Characterization |
| Charge Transfer Traps | PSF Fitting Photometry |
| Chip-to-Chip Normalization | PSF Subtraction |
| Completeness Corrections | Quad Filters |
| Cosmic Rays | Recalibration |
| CTE Losses | Red Leaks |
| Darks | Residual Images |
| Data Quality | Saturated Data |
| Deconvolution | Scattered Light |
| Dithering | Serial Clocks |
| Drizzle | Size Measurements |
| Field Distortion | Software |
| Flats | Surface Photometry |
| Focus | SYNPHOT |
| Hot Pixels | T=77 Observations |
| Image Anomalies | UV Throughput |
| Linear Ramp Filters | Vignetting |
| Long vs. Short Exposures | Woods Filters |
| Narrow Band Photometry | 1997 Servicing Mission |

# Updates to System Efficiencies and Zeropoints

***To be read in conjunction with Section 6.1 of the*** *WFPC2 Instrument Handbook,* ***Version 4.0.***

Table 1.2 on page 22 is an update to Table 6.1 of the *WFPC2 Instrument Handbook*. New calibration information has caused us to update the estimated efficiencies and throughputs of several of the narrow-band and UV filters since the last publication of this table. These numbers are accurate to at least 10%—which is sufficient for planning observations, but

not for the analysis of many programs. Investigators wishing to do photometry on WFPC2 images should refer to the *HST Data Handbook* for an explanation of the conventions used in determining WFPC2 zeropoints and should use the zeropoints given in Table 28.1 of the Data Handbook. For the most accurate and up-to-date calibrations, users should examine the on-line version of the Data Handbook to verify that no numbers of interest have changed since the last paper publication.

Table 1.2: System Efficiencies and Zeropoints. Replaces Table 6.1 in the Instrument Handbook, Version 4.0 (see original table for definitions).

| Filter | $\int QT d\lambda/\lambda$ | $\lambda$ | $\delta\lambda$ | $\sigma$ | $QT_{max}$ | $d\lambda/d\alpha$ | $\lambda_p$ | $<\lambda>$ | $\lambda_{max}$ | $m_{e/sec}$ | $t_{wfsky}$ |
|---|---|---|---|---|---|---|---|---|---|---|---|
| F122M | 0.00011 | 1356.2 | 1070.3 | 0.3350 | 0.00107 | 152.25 | 1827.4 | 2147.7 | 1260 | 18.62 | 1.1E+07 |
| F130LP | 0.10175 | 4285.0 | 4755.4 | 0.4713 | 0.13936 | 951.67 | 5814.6 | 6137.5 | 6390 | 26.01 | 1.9E+02 |
| F160BW | 0.00024 | 1472.9 | 449.3 | 0.1295 | 0.00074 | 24.72 | 1521.7 | 1534.7 | 1400 | 19.46 | 9.2E+05 |
| F165LP | 0.10091 | 4493.9 | 4528.8 | 0.4280 | 0.14066 | 823.04 | 5852.9 | 6155.6 | 6400 | 26.00 | 1.9E+02 |
| F170W | 0.00057 | 1714.7 | 695.3 | 0.1722 | 0.00169 | 50.84 | 1838.2 | 1891.8 | 1858 | 20.39 | 2.3E+06 |
| F185W | 0.00038 | 1944.8 | 379.9 | 0.0829 | 0.00196 | 13.38 | 1973.4 | 1982.5 | 1940 | 19.94 | 7.3E+06 |
| F218W | 0.00059 | 2178.2 | 405.5 | 0.0791 | 0.00286 | 13.61 | 2205.7 | 2213.0 | 2242 | 20.42 | 5.4E+06 |
| F255W | 0.00080 | 2578.2 | 402.4 | 0.0663 | 0.00462 | 11.33 | 2601.0 | 2606.9 | 2537 | 20.76 | 2.6E+06 |
| F300W | 0.00571 | 2920.9 | 766.5 | 0.1115 | 0.01974 | 36.28 | 2994.3 | 3015.1 | 2805 | 22.89 | 6.7E+04 |
| F336W | 0.00498 | 3332.2 | 478.8 | 0.0610 | 0.03558 | 12.41 | 3359.2 | 3368.4 | 3454 | 22.74 | 3.6E+04 |
| F343N | 0.00003 | 3425.9 | 212.6 | 0.0263 | 0.00397 | 2.38 | 3431.9 | 3434.4 | 3432 | 17.27 | 4.7E+06 |
| F375N | 0.00008 | 3730.8 | 239.5 | 0.0273 | 0.00983 | 2.77 | 3737.7 | 3740.3 | 3736 | 18.24 | 1.1E+06 |
| F380W | 0.00779 | 3940.5 | 682.0 | 0.0735 | 0.03753 | 21.29 | 3982.7 | 3993.1 | 4000 | 23.22 | 7.1E+03 |
| F390N | 0.00031 | 3888.1 | 117.9 | 0.0129 | 0.01999 | 0.64 | 3889.8 | 3890.3 | 3890 | 19.72 | 2.1E+05 |
| F410M | 0.00183 | 4088.4 | 219.4 | 0.0228 | 0.04027 | 2.12 | 4092.6 | 4094.0 | 4098 | 21.65 | 2.7E+04 |
| F437N | 0.00022 | 4369.1 | 59.1 | 0.0057 | 0.03065 | 0.14 | 4369.5 | 4369.5 | 4368 | 19.37 | 1.7E+05 |
| F439W | 0.00576 | 4292.7 | 476.2 | 0.0471 | 0.03904 | 9.53 | 4311.6 | 4316.4 | 4318 | 22.90 | 7.1E+03 |
| F450W | 0.01679 | 4483.6 | 951.6 | 0.0901 | 0.08675 | 36.42 | 4555.6 | 4573.1 | 5068 | 24.06 | 2.0E+03 |
| F467M | 0.00250 | 4667.7 | 177.9 | 0.0162 | 0.05583 | 1.22 | 4670.2 | 4670.9 | 4732 | 21.99 | 1.2E+04 |
| F469N | 0.00027 | 4694.4 | 42.1 | 0.0038 | 0.03784 | 0.07 | 4694.5 | 4694.6 | 4698 | 19.56 | 1.1E+05 |
| F487N | 0.00034 | 4865.0 | 75.1 | 0.0066 | 0.04811 | 0.21 | 4865.3 | 4865.2 | 4864 | 19.81 | 8.1E+04 |
| F502N | 0.00041 | 5012.7 | 113.5 | 0.0096 | 0.05800 | 0.46 | 5013.0 | 5012.8 | 5010 | 20.04 | 5.9E+04 |
| F547M | 0.01342 | 5467.9 | 484.0 | 0.0376 | 0.11516 | 7.73 | 5483.3 | 5487.1 | 5560 | 23.81 | 1.6E+03 |
| F555W | 0.03012 | 5337.9 | 1228.7 | 0.0977 | 0.11194 | 51.00 | 5439.0 | 5464.7 | 5550 | 24.69 | 7.3E+02 |

Table 1.2: System Efficiencies and Zeropoints. Replaces Table 6.1 in the Instrument Handbook, Version 4.0 (see original table for definitions).

| Filter | $\int$ QTd $\lambda/\lambda$ | $\lambda$ | $\delta\lambda$ | $\sigma$ | $QT_{max}$ | $d\lambda/d\alpha$ | $\lambda_p$ | $<\lambda>$ | $\lambda_{max}$ | $m_{e/sec}$ | $t_{wfsky}$ |
|---|---|---|---|---|---|---|---|---|---|---|---|
| F569W | 0.02343 | 5582.0 | 966.4 | 0.0735 | 0.11518 | 30.17 | 5642.0 | 5657.6 | 5550 | 24.42 | 8.9E+02 |
| F588N | 0.00145 | 5894.0 | 80.5 | 0.0058 | 0.13078 | 0.20 | 5893.5 | 5893.7 | 5896 | 21.40 | 1.3E+04 |
| F606W | 0.04513 | 5894.0 | 1502.5 | 0.1089 | 0.14221 | 69.47 | 5996.8 | 6030.9 | 6188 | 25.13 | 4.2E+02 |
| F622W | 0.02882 | 6137.1 | 917.5 | 0.0635 | 0.14096 | 24.74 | 6186.3 | 6198.6 | 6404 | 24.64 | 6.3E+02 |
| F631N | 0.00084 | 6306.4 | 30.8 | 0.0021 | 0.12632 | 0.03 | 6306.4 | 6306.5 | 6302 | 20.81 | 2.1E+04 |
| F656N | 0.00049 | 6562.7 | 127.9 | 0.0083 | 0.11273 | 0.45 | 6563.6 | 6563.7 | 6562 | 20.21 | 3.5E+04 |
| F658N | 0.00068 | 6590.6 | 69.9 | 0.0045 | 0.11443 | 0.13 | 6590.9 | 6591.0 | 6592 | 20.58 | 2.5E+04 |
| F673N | 0.00113 | 6731.7 | 72.8 | 0.0046 | 0.11978 | 0.14 | 6732.2 | 6732.3 | 6730 | 21.12 | 1.4E+04 |
| F675W | 0.02344 | 6677.1 | 867.7 | 0.0552 | 0.13613 | 20.34 | 6717.4 | 6727.6 | 6636 | 24.42 | 7.0E+02 |
| F702W | 0.03429 | 6817.6 | 1384.8 | 0.0863 | 0.14186 | 50.72 | 6918.5 | 6944.3 | 6512 | 24.83 | 4.6E+02 |
| F785LP | 0.00900 | 8627.5 | 1381.3 | 0.0680 | 0.04831 | 39.88 | 8707.0 | 8727.5 | 8224 | 23.38 | 1.3E+03 |
| F791W | 0.01694 | 7810.8 | 1231.5 | 0.0670 | 0.09531 | 35.02 | 7880.6 | 7898.4 | 7400 | 24.07 | 7.6E+02 |
| F814W | 0.01949 | 7904.6 | 1539.7 | 0.0827 | 0.10344 | 54.08 | 8012.2 | 8040.3 | 7260 | 24.22 | 6.5E+02 |
| F850LP | 0.00473 | 9086.2 | 1037.5 | 0.0485 | 0.03939 | 21.37 | 9128.8 | 9139.8 | 8810 | 22.68 | 2.4E+03 |
| F953N | 0.00016 | 9544.8 | 52.5 | 0.0023 | 0.02213 | 0.05 | 9544.9 | 9545.0 | 9526 | 19.00 | 6.9E+04 |
| F1042M | 0.00017 | 10209.7 | 630.8 | 0.0262 | 0.00481 | 7.03 | 10225.0 | 10228.0 | 10110 | 19.10 | 6.0E+04 |
| FQUVN-A | 0.00033 | 3763.9 | 74.5 | 0.0084 | 0.01327 | 0.27 | 3764.5 | 3764.6 | 3802 | 19.78 | 2.5E+05 |
| FQUVN-B | 0.00030 | 3828.6 | 91.0 | 0.0101 | 0.01557 | 0.39 | 3829.4 | 3829.5 | 3828 | 19.68 | 2.4E+05 |
| FQUVN-C | 0.00037 | 3912.0 | 85.7 | 0.0093 | 0.01900 | 0.34 | 3912.9 | 3913.0 | 3910 | 19.92 | 1.7E+05 |
| FQUVN-D | 0.00047 | 3991.2 | 90.4 | 0.0096 | 0.02330 | 0.37 | 3992.1 | 3992.2 | 3990 | 20.17 | 1.2E+05 |
| FQCH4N-A | 0.00076 | 5438.9 | 295.9 | 0.0231 | 0.09537 | 2.90 | 5445.6 | 5447.8 | 5442 | 20.70 | 2.9E+04 |
| FQCH4N15-B | 0.00088 | 6207.0 | 377.9 | 0.0259 | 0.12242 | 4.15 | 6215.4 | 6218.2 | 6202 | 20.86 | 2.0E+04 |
| FQCH4N33-B | 0.00091 | 6206.9 | 370.3 | 0.0253 | 0.12543 | 3.99 | 6214.7 | 6217.5 | 6202 | 20.89 | 2.0E+04 |
| FQCH4N-C | 0.00070 | 7282.6 | 341.9 | 0.0199 | 0.10275 | 2.90 | 7288.9 | 7290.3 | 7278 | 20.61 | 2.1E+04 |
| FQCH4N-D | 0.00023 | 8886.2 | 502.5 | 0.0240 | 0.02917 | 5.12 | 8896.7 | 8898.7 | 8930 | 19.40 | 5.0E+04 |
| POLQ_par | 0.06005 | 5570.9 | 4184.5 | 0.3190 | 0.09298 | 566.81 | 6076.2 | 6323.3 | 6476 | 25.44 | |
| POLQ_per | 0.01299 | 7027.7 | 5153.2 | 0.3114 | 0.03744 | 681.43 | 7541.1 | 7766.0 | 7839 | 23.78 | |

# WFPC2 Calibration Plan

***To be read in conjunction with Section 8.10 of the*** *WFPC2 Instrument Handbook****, Version 4.0.***

## Introduction

In this section we discuss the Cycle 7 and 8 calibration plans for WFPC2. It is the policy of the Institute to attempt to obtain the necessary calibration files for the vast majority of user programs. In some cases, however, users may find that they will need to take calibration images as part of their program. If there is any doubt about the suitability of the present calibrations for a specific program, please feel free to contact the WFPC2 group via E-mail to `help@stsci.edu`.

The results of the calibration programs are reported to users through the *HST Data Handbook* for results of general interest, and also through frequent Instrument Science Reports available from the STScI on-line information service. HST users should rely on these, rather than the Instrument Handbook, when the most accurate, up-to-date numbers are required.

## Overview

The main goals of the WFPC2 Calibration Plans for Cycles 7 and 8 are:

- verify that the instrument remains stable in its main characteristics.
- address its photometric accuracy.
- follow the long-term changes that are appearing in the instrument after 5 years of on-orbit service.

These goals are achieved by a mix of monitoring programs, which verify the stability and continued performance of the camera by repeating routine observations on a regular basis, and special calibrations, which have the goal to enhance the WFPC2 calibration in specific areas.

### Standard Monitoring Programs

The stability of WFPC2 is mainly verified through the Photometric Monitoring program and the set of internal monitoring programs. Starting in Cycle 8, several of these monitors - whose execution is linked to the periodic decontaminations of the camera - have been merged into a common program together with the decontaminations themselves (programs 8441, 8459), in order to facilitate their scheduling.

The Photometric Monitoring program (7618, 8441, 8459) consists of regular one-orbit visits of our photometric standard GRW+70d5824, executed immediately before and after decontaminations. These observations allow us to monitor efficiently four main areas: the overall photometric throughput of the camera, the contamination of the CCD windows, especially in the UV, the PSF properties at different wavelengths, and the OTA focus. We continue to rely heavily on internal observations for some instrument maintenance and for many other types of monitoring: decontaminations (7619, 8441, 8459) to clear the contaminants from the CCD windows and to limit the growth in hot pixels; darks (7620, 8442) in order to produce up-to-date, high-quality dark reference files and to identify new hot pixels in a timely manner; biases, INTFLATs, and K-spots (decontamination programs, plus 7622, 7623, and 8444, 8448), to verify the integrity of the camera's optics and electronics chain, and the pixel-to-pixel response in the visible; Earth Flats (7625, 8445) to follow variations in the large-scale flatfield; and UV flats using the internal UV lamp (7624 8449), to monitor the pixel-to-pixel response in the UV. The planned observations have remained largely the same as in previous cycles, except that internal flats place an increasing emphasis on the INTFLAT channel because of the continuing degradation of the VISFLAT channel.

### Other Monitoring Programs

Some additional monitoring programs introduced in Cycles 7 and 8 deserve special mention. The Supplemental Darks program (7621, 7712, 7713, 8443, 8460, 8461) aims at obtaining a large number of relatively short darks on a very frequent basis, with the main goal of helping users identify hot pixels in their observations. The program has been designed to place the least possible burden on the scheduling system; that these additional darks have a low priority, and are scheduled whenever feasible. Under normal circumstances, this program provides up to 21 additional 1000s darks per week, thus giving users a good chance of having a dark within half a day of their observations. The Astrometric Monitor program (7627, 8446) measures the relative placement of the four WFPC2 CCD in the focal plane; we have evidence that shifts of up to 150 mas have occurred since 1994, and the Astrometric Monitor program is designed to track the continuing motion of the detectors. Finally, the CTE Monitor (7929, 8447), introduced late in Cycle 7, measures the photometric impact of the loss in charge transfer efficiency of the WFPC2 detectors, which continues to increase with time.

### Special Calibration Programs

Special calibration programs address specific areas of WFPC2 calibration that require dedicated calibration measurements. They include substantial photometric, CTE and PSF characterization programs, of interest to the majority of WFPC2 users, as well as a number of smaller programs which address areas of more limited interest.

The Photometric Characterization program, a continuation of the Cycle 6 program of the same name, is designed to improve the link between WFPC2 and ground-based photometry. The Cycle 7 program (7628) includes additional observations of NGC 2100, a young LMC cluster, and NGC 2419, a very distant globular cluster in the Milky Way, which allows good coverage of the bright red giants, too bright and rare in nearby clusters. We also carry out a filter sweep on both our primary standard, GRW+70d5824, and our reference rich field in ω Cen. In Cycle 8 (8451) we repeat the filter sweep of the primary standard.

The Cycle 7 CTE Characterization program (7630) has provided a thorough exploration of the various parameters that could affect the so-called “long vs. short” anomaly, that is, the observed difference in count rates between long and short exposures. This extensive set of dedicated observations, in which each of the potentially critical parameters is varied in turn, has enabled us to characterize the anomaly and to suggest a correction formula that removes its impact almost completely. Two Cycle 8 programs (8450, 8456), described below, address the viability of noiseless preflash and the CTE effect on extended sources.

The PSF Characterization program (7629) continues our accumulation of data for the WFPC2 PSF library, by addressing often-used filters such as F300W, F450W, F702W which were not included in previous cycles. In Cycle 8 (8452) we repeat the measurements for F555W and F814W only.

In Cycle 8 we started several new special calibration programs, mostly to address special interest areas that had not been covered adequately in previous cycles. The Noiseless Preflash test (8450), already mentioned, will determine whether illuminating the detectors prior to an exposure might reduce the impact of its known photometric anomalies. This is a revised and improved version of the test carried out as part of the CTE Characterization program, which proved insufficient to establish the viability of this technique. The CTE Test for Extended Sources (8456) will verify to what extent the CTE impacts the photometry of faint, extended sources such as distant galaxies. The Plate Scale Verification (8458) will measure the effective plate scale of WFPC2 through several filters, with special emphasis on the far UV. The Photometry of Very Red Stars (8455) will verify the WFPC2 photometric calibration and determine color terms for very red (late M) stars. The UV Earth Flats (8457) will produce higher-quality flatfields for UV filters, whose quality is currently limited by the low signal levels in the internal flatfield calibration. Finally, we will repeat part of the Polarization (8453) and the Linear Ramp Filter (8454) calibrations, in order to both verify and complete our calibrations of these special modes.

We now present a summary description of each calibration program, with a statement of the purpose of the program and of how it will be carried out, plus indications of the expected products. The desired and expected accuracy of each program is also explicitly stated. Table 1.3 on page 28

summarizes the relevant data for Cycle 7 programs, and Table 1.4 on page 37 those for Cycle 8.

Electronic versions of the calibration plans are available via the World Wide Web at:

http://www.stsci.edu/instruments/wfpc2/wfpc2_bib.html

Details on individual proposals can be found through the HST Program Information page at URL

http://presto.stsci.edu/public/propinfo.html

Table 1.3: WFPC2 Cycle 7 Calibration Plan

| ID | Proposal Title | Frequency | Estimated Time (orbits) | | Products | Accuracy | Notes |
|---|---|---|---|---|---|---|---|
| | | | "External" | "Internal" | | | |
| **Routine Monitoring Programs** | | | | | | | |
| 7618 | Photometric Monitor | 1–2/4 weeks | 36 | | SYNPHOT | 1–2% | Also focus monitor |
| 7619 | Decontamination | 1/4 weeks | | 288 | CDBS | n/a | Used together with darks, internals |
| 7620 | Standard Darks | weekly | | 360 | CDBS, WWW | 1 e/hr | Also hot pixel lists on WWW |
| 7621, 7712, 7713 | Supplemental Darks | weekly | | 2016 | | n/a | No analysis provided |
| 7622 | Internal Monitor | 2/4 weeks | | 72 | CDBS, TIR | 0.8 e/pixel | New superbias (with 7619) |
| 7623 | Internal Flats | 1/4 weeks | | 75 | TIR | 0.3% | Mostly INTFLATs |
| 7624 | UV Flatfield Monitor | 2/cycle | 4 | 8 | | 2-8% | Before and after decon |
| 7625 | Earth Flats | continuous | | 155 | CDBS | 0.3% | Also LRF, Methane quads |
| 7626 | UV Throughput | 2/cycle | 4 | | SYNPHOT | 3–10% | |
| 7627 | Astrometric Monitor | 2/cycle | 2 | 2 | TIPS, TIR | 0.″05 | Also K-spots |
| **Special Calibration Programs** | | | | | | | |
| 7628 | Photometric Characterization | 1 | 10 | | ISR | 2–5% | Also test zeropoint differences between chips, UV vignetting, astrometry |
| 7629 | PSF Characterization | 1 | 5 | | WWW | 10% | Covers widely used, high-throughput filters |
| 7630 | CTE Characterization | 1 | 14 | | ISR | 0.01 mag | Extensive coverage of preflash levels and exposure times in F555W, spot checks in F555W, F300W, hysteresis, CTE ramp |
| 7929 | CTE Monitor | 4 | 4 | | ISR | 0.02 mag | Measure changes in CTE ramp |
| 8053 | Supplemental Earth Flats | 1 | | 155 | CDBS | 0.3% | Repeat Earth Flats towards end of cycle |
| 8054 | LRF Calibration | 1 | 10 | | ISR | 3–5% | Complete LRF calibration, test stability |
| TOTAL TIME (including all executions) | | | 89 | 3131 | | | |

### Proposal ID 7618: WFPC2 Cycle 7: Photometric Monitor

**Purpose**: Regular external check of instrumental stability. Based on Cycle 6 program 6902.
**Description**: The standard star GRW+70d5824 is observed before and after a decontamination using three different strategies:

- F170W in all four chips to monitor contamination in the far UV.
- F439W, F555W, F814W on the PC to monitor focus.
- F160BW, F218W, F255W, F300W, F336W, F439W, F555W, F675W, F814W in a different chip each month. Some filters may be cut because of lack of time.

Observations are taken after each decontamination and before every other decontamination, resulting in 36 orbits for 24 decontamination cycles.
**Accuracy**: Overall discrepancies between the results of this test need to be measured to better than 2% and are expected to be less than 1% rms. This has been the case in Cycles 4 through 6. The point of the test is to measure this variation. Focus measurements have an expected accuracy of 1.5 micron, and a goal of 1 micron; the uncertainty in the focus determination is dominated by external factors, such as OTA breathing.
**Products**: Instrument Handbook, reports at monthly TIPS meetings, WWW (sensitivity trends); updates in UV sensitivity variation used in SYNPHOT.

### Proposal ID 7619: WFPC2 Cycle 7: Decontamination

**Purpose**: UV blocking contaminants are removed, and hot pixels cured, by warming the CCDs to +20C for six hours.
**Description**: The decontamination itself is implemented via the DECON mode, in which the TECs are turned off and the CCD and heatpipe heaters are turned on to warm the detectors and window surfaces. Keeping WFPC2 warm for ~6 hours has been shown in previous Cycles to be sufficient to remove the contaminants and anneal many hot pixels.
The internal observations taken before and after each decontamination consist of: 4 biases (2 at each gain setting), 4 INTFLATs (2 at each gain setting), 2 K-spots (both at gain 15, one short and one long exposure, optimized for PC and WF), and finally, 5 darks (gain 7, clocks off). To minimize time-dependent effects, each set of internals will be grouped within 2 days and performed no more than 1 day before the decon and no later that 12 hours after the decon. To protect against residual images in the darks (which results in the irretrievable loss of the critical pre-decon hot pixel status), the darks will be executed as a non-interruptible sequence at least 30 minutes after any other WFPC2 activity.
**Accuracy**: This proposal is mainly designed to maintain the health of the instrument. Biases, darks and other internals taken with this proposal are

used in generating appropriate reference files (see Proposals 7620 and 7622).
**Products**: Those obtained from use of darks, biases and other internals (see Proposals 7620 and 7622).

### Proposal ID 7620: WFPC2 Cycle 7: Standard Darks

**Purpose**: Measure dark current on individual pixels and identify hot pixels at frequent intervals.
**Description:** Every week, five 1800s exposures are taken with the shutter closed. The length of the exposures is chosen to fit nicely within an occultation period. The weekly frequency is required because of the high formation rate of new hot pixels (several tens per CCD per day). Five darks a week are required for cosmic ray rejection, to counterbalance losses due to residual images, and to improve the noise of individual measurements. Even with these measures, some weeks no usable darks will be available because of residual images. Normally this results only in a longer-than-usual gap in the hot pixel lists, but in a decontamination week, information on pixels that became hot and then annealed would be lost irretrievably. For this reason, pre-decon darks are to be executed in a non-interruptible sequence, at least 30 minutes after any WFPC2 activity (see Proposal 7619). Normal darks do not need to be protected in this fashion. The Supplemental Darks program (7621, 7712, 7713) will provide additional information on hot pixels.
**Accuracy**: The required accuracy for darks is about 1 $e^-$/hour (single-pixel rms) for the vast majority of science applications. The expected accuracy in a typical superdark is 0.05 $e^-$/hour for normal pixels. The need for regular dark frames is driven by systematic effects, such as dark glow (a spatially and temporally variable component of the dark signal) and hot pixels, which cause errors that may exceed these limits significantly.
**Products**: Weekly dark frames delivered to CDBS and monthly tables of hot pixels on the Web.

### Proposal ID 7621, 7712, 7713: WFPC2 Cycle 7: Supplemental Darks

**Purpose**: Obtain very frequent monitoring of hot pixels.
**Description**: This program is designed to provide up to three short (1000s) darks per day, to be used primarily for the identification of hot pixels. Shorter darks are used so that observations can fit into almost any occultation period, making automatic scheduling feasible. Supplemental darks will be taken at low priority, and only when there is no other requirement for that specific occultation period. This program is complementary with 7620, Standard Darks, whose longer individual observations are better suited to produce high-quality pipeline darks and superdarks, and are also carried out at higher priority. Note that hot pixels are often a cause of concern for relatively short science programs, since they can mimic or mask key features of the observations, and about 400

new hot pixels per CCD are formed between executions of the Standard Darks program (7620). These observations will be made available as a service to the GO community, and there is no plan to use them in our standard analysis and products. This program has become feasible starting in Cycle 7, due to the placement of a solid state recorder on-board HST.
**Accuracy**: N/A
**Products**: None

### Proposal ID 7622: WFPC2 Cycle 7: Internal Monitor

**Purpose**: Verification of short-term instrument stability for both gain settings.
**Description**: The internal observations will consist of 8 biases (4 at each gain) and 4 INTFLATs (2 at each gain). The entire set should be run once per week, except for decon weeks, on a non-interference basis. This proposal is similar to the Cycle 6 Internal Monitor (6905).
**Accuracy**: Approximately 120 bias frames will be used for each superbias pipeline reference file, generated once a year; accuracy is required to be better than 1.5 $e^-$/pixel, and is expected to be 0.8 $e^-$/pixel.
**Products**: Superbiases delivered yearly to CDBS; TIPS reports on possible buildup of contaminants on the CCD windows (worms) as well as gain ratio stability, based on INTFLATs. A Technical Instrument Report will be issued if significant changes occur.

### Proposal ID 7623: WFPC2 Cycle 7: Internal Flats

**Purpose**: Monitor the pixel-to-pixel flatfield response and the VISFLAT lamp degradation as well as detect any possible changes due to contamination. This program is a combination and continuation of the Cycle 6 VISFLAT Monitor and INTFLAT Monitor proposals (6906, 6907, respectively). The VISFLAT portion has been minimized to conserve the lifetime of the CAL channel lamp.
**Description**: This proposal contains an INTFLAT filter sweep, a VISFLAT mini-sweep, linearity tests, and monitoring images. Monitoring is carried out by taking INTFLATs with the photometric filter set after each decon. The VISFLAT mini-sweeps (before and after decon, twice during the cycle) will include the photometric filter set at gain 7, plus the linear ramp filter FR533N at both gains to test the camera linearity. The INTFLAT sweep, taken within a two-week period, includes almost all filters, some with both blades and gains (F336W, F439W, F547M, F555W, F569W, F606W, F622W, F631N, F502N, F656N, F675W, F673N, F702W, F785LP, F814W, F1042M), others with just one blade and gain (F487N, F467M, F588N, F380W, F658N, F791W, F850LP, F953N, F450W, F300W, F390N, F410M, F437N, F469N, and F160BW). The linearity test is done at both gains and blades using F555W, and an additional set with one blade and gain with clocks on.
**Accuracy**: Assuming Cycle 7 results will be similar to those from previous cycles, the VISFLATs should be stable to better than 1%, both in overall

level and spatial variations (after correcting for lamp degradation), and contamination effects should be < 1%. For the INTFLATs, the signal-to-noise ratio per pixel is estimated to be similar to the VISFLATs, but the spatial and wavelength variations in the illumination pattern are much larger. However, the INTFLATs will provide a baseline comparison of INTFLAT vs. VISFLAT, in the event of a complete failure of the CAL channel system. Temporal variations in the flatfields can be monitored at the 1% level. Gain ratios should be stable to better than 0.1%.
**Products**: TIPS report, Technical Instrument Report if any significant variations are observed.

### Proposal ID 7624: WFPC2 Cycle 7: UV Flatfield Monitor

**Purpose**: Monitor the stability of UV flatfield.
**Description**: UV flatfields will be obtained with the CAL channel's ultraviolet lamp (UVFLAT) using the UV filters F122M, F170W, F160BW, F185W, and F336W. The UV flats will be used to monitor UV flatfield stability and the stability of the Woods filter (F160BW) by using F170W as the control. The F336W ratio of VISFLAT (Cycle 6 proposal 6906) to UVFLAT will provide a diagnostic of the UV flatfield degradation and tie the UVFLAT and VISFLAT flatfield patterns together. Two supplemental dark frames must be obtained immediately after each use of the lamp, in order to check for possible after-images.
**Accuracy**: About 2-8% pixel-to-pixel expected (depending on filter).
**Products**: New UV flatfields if changes are detected.

### Proposal ID 7625: WFPC2 Cycle 7: Earth Flats

**Purpose**: Monitor flatfield stability.
**Description**: As in Cycle 6 program 6909, sets of 200 Earth-streak flats are taken to construct high quality narrow-band flatfields with the filters F160BW, F375N, F502N, F656N and F953N. Of these 200 perhaps 50 will be at a suitable exposure level for destreaking. The resulting Earth superflats map the OTA illumination pattern and will be combined with SLTV data (and calibration channel data in case of variation) for the WFPC2 filter set to generate a set of superflats capable of removing both the OTA illumination and pixel-to-pixel variations in the flatfields. The general plan of Cycles 5 and 6 is repeated.
**Accuracy**: The single-pixel signal-to-noise ratio expected in the flatfield is 0.3%.
**Products**: New flatfields to CDBS if any changes are detected.

### Proposal ID 7626: WFPC2 Cycle 7: UV Throughput

**Purpose**: Verify throughput for all UV filters. Loosely based on the Cycle 5 and 6 UV throughput proposals (6186, 6936).
**Description**: GRW+70d5824 will be observed shortly before and after a DECON through all the UV filters in PC and WF3. Observations should be taken roughly mid-way through the cycle.

**Accuracy**: The UV throughput will be measured to better than 3%.
**Products**: TIPS, SYNPHOT update if necessary, Technical Instrument Report to document any changes if necessary.

### Proposal ID 7627: WFPC2 Cycle 7: Astrometric Monitor

**Purpose**: Verify relative positions of WFPC2 chips with respect to one another. Repeats parts of Cycle 6 proposal 6942 twice during Cycle 7.
**Description**: The rich field in ω Cen used for the Astrometry Verification (6942) is observed with large shifts (35″) in F555W only, at two different times during Cycle 7. This will indicate whether there are shifts in the relative positions of the chips or changes in the astrometric solution at the subpixel level. Kelsall spot images will be taken in conjunction with each execution. The K-spots data and some external data indicate that shifts of up to 1 pixel may have occurred since mid-1994.
**Accuracy**: At least 0.″1 in the relative shifts, with a goal of 0.″02–0.″05.
**Products**: TIPS, Technical Instrument Report; update of chip positions in PDB and of geometric solution in STSDAS task **metric** if any changes are found.

### Proposal ID 7628: WFPC2 Cycle 7: Photometric Characterization

**Purpose**: (1) Determine whether any changes in the zeropoint, or in the spatial dependence of the zeropoint or contamination, have occurred; (2) include another globular cluster (NGC 2419) in order to extend the parameter space for determinations of photometric transformation. Combines and continues Cycle 6 proposals 6934, 6935.
**Description**: Observations of the primary photometric standard GRW+70d5824 will be compared against baseline observations. The cluster fields in ω Cen and NGC 2100 will be compared to previously obtained data in order to test for spatial variations in the throughput. Most broad-band and intermediate-width filters, including the far UV set for NGC 2100 (very young, many blue stars). A contamination test using UV filters will also be performed for NGC 2100. New observations of the Galactic globular cluster NGC 2419 will be compared with good ground-based photometry; this cluster is very distant (100 kpc) and will provide a large color spread on giant branch and HB.
**Accuracy**: Photometric stability expected to be better than 2%. Photometric transformations to be defined to 2–5%, depending on filter; most of the error derives from limited knowledge of the transformations between ground-based and WFPC2 photometric systems.
**Products**: ISR; SYNPHOT updates if necessary.

### Proposal ID 7629: WFPC2 Cycle 7: PSF Characterization

**Purpose**: Provide a subsampled PSF over the full field to allow PSF fitting photometry, test PSF subtraction as well as dithering techniques. Based on Cycle 6 program 6938.

**Description**: Measure the PSF over the full field in often-used, high-throughput filters in order to update the Tim and TinyTim models and to allow accurate empirical PSFs to be derived for PSF fitting photometry. Compared to Cycles 5 and 6, we will repeat F814W to provide a continuing baseline, and will replace the other filters with F300W, F450W, F606W and F702W, which are often used because of their high throughput but are not as well characterized as the photometric set (F336W, F439W, F555W, F675W) used in previous Cycles. These observations will also be useful in order to test PSF subtraction and dithering techniques at various locations on the CCD chips. With one orbit per photometric filter, a spatial scan is performed over a 4 x 4 grid on the CCD. The step size is 0.025 arcseconds; this gives a critically sampled PSF over most of the visible range. This program uses the same specially chosen field in ω Cen as the Cycle 5 proposal 6193. The proposal also allows a check for sub-pixel phase effects on the integrated photometry.
**Accuracy**: Provides measurement of pixel phase effect on photometry (sub-pixel QE variations exist). The chosen field will have tens of well exposed stars in each chip. Each star will be measured 16 times per filter at different pixel phase. The proposal therefore provides, in principle, a high signal-to-noise, critically sampled PSF. This will improve the quality of PSF fitting photometry for the filters used. The result will be largely limited by breathing variations in focus. It is difficult to predict the PSF accuracy that will result. If breathing is less than 5 microns peak-to-peak, the resulting PSFs should be good to about 10% in each pixel. In addition, the test gives a direct measurement of sub-pixel phase effects on photometry, which should be measured to better than 1%.
**Products**: PSF library (WWW).

### Proposal ID 7630: WFPC2 Cycle 7: CTE Calibration

**Purpose**: Conduct a thorough examination of the variation in photometric zeropoint as a function of exposure length, background (via preflash), and position in the chip. Include spot checks for the dependence of zeropoint variations on filter, order of exposures, and camera shifts (CTE ramp).
**Description**: A well-studied field in the globular cluster NGC 2419 will be observed through F814W with a combination of exposure times (10, 40, 100, 300, 1000s) and preflash levels (0, 5, 10, 100, and 1000 $e^-$). Completes Cycle 6 proposal 6937, which was shortened substantially because of SM constraints. Will also include several observations in reverse order (to test for hysteresis), in F555W and F300W (filter dependence), and after a pointing shift (to test for x, y dependence), as well as a series of equal-length exposures to test the effect of noiseless preflash. This proposal should improve substantially our understanding of CTE and of the long vs. short anomaly.
**Accuracy**: The reported short vs. long effect is ~0.05 mag. We want to determine it to better than 0.02 mag, with a goal of 0.01 mag.

**Products**: ISR, paper; if appropriate, a special task to correct the CTE effect will be generated.

### Proposal ID 7929: WFPC2 Cycle 7: CTE Monitor

**Purpose**: Monitor variations in CTE ramp for bright and faint targets.
**Description**: Analysis of Cycle 6 CTE data shows that the CTE ramp depends strongly on stellar magnitude and background, and that its amplitude varies in time for faint stars. However, most measurements have been taken so far under slightly different conditions from one another. This program will take four one-orbit measurements of the CTE at four month intervals, under the same conditions as the best data taken so far. It will provide an accurate and efficient tracer of changes in the CTE ramp, and show to what extent WFPC2 remains a photometric instrument for faint objects. Observations of the standard field in NGC 5139 (ω Cen) will be taken at the same roll angle, but centered in each of the WF chips in turn, thus reversing the x and y positions of each star. No preflash test is included.
**Accuracy**: The measurements will enable tracking of the CTE ramp with an accuracy requirement of 0.02 mag, and a goal of 0.01 mag.
**Products**: ISR.

### Proposal ID 8053: WFPC2 Cycle 7: Supplemental Earth Flats

**Purpose**: Repeat the sequence of Earth Flats late in Cycle 7 to verify stability of flatfield.
**Description**: As in previous cycles and earlier in Cycle 7, sets of 200 Earth-streak flats are taken to construct high quality narrow-band flatfields with the filters F160BW, F375N, F502N, F656N and F953N. Of these 200 perhaps 50 will be at a suitable exposure level for destreaking. The resulting Earth superflats map the OTA illumination pattern and will be combined with SLTV data (and calibration channel data in case of variation) for the WFPC2 filter set to generate a set of superflats capable of removing both the OTA illumination and pixel-to-pixel variations in the flatfields. A repeat is requested because of the length of Cycle 7 and the fact that low-level temporal variations are typically discerned on time scales of about a year.
**Accuracy**: Large-scale flatfield variations can be tracked to about 0.3%.
**Products**: New flatfields will be generated and delivered.

### Proposal ID 8054: WFPC2 Cycle 7: LRF Calibration

**Purpose**: Complete the analysis of LRF properties: throughput and wavelength scale.
**Description**: The primary spectrophotometric standard GRW+70d5824 will be observed at several locations on the three most used Linear Ramp Filters to verify its throughput as a function of wavelength. In addition, exposures of the Orion Nebula at two different pointings will be used to verify the wavelength calibration of the LRF at the wavelengths of major

nebular lines. Previous executions of the LRF calibration have demonstrated a throughput consistent with the expectations based on laboratory filter tracings, with a scatter of 8% rms. The series of observations of GRW+70d5824 will: 1) measure the temporal stability of the difference between measured and predicted throughput; 2) demonstrate whether the scatter is due to measurement errors or to intrinsic variations in the filter; 3) complete the wavelength coverage (some of the observations from previous programs were lost); and 4) and provide more closely spaced points in the most often used ramp filter. The observations of the Orion Nebula, at two carefully optimized pointings, will provide a direct test of the wavelength calibration and vignetting of the LRF at the wavelengths of Hα, Hβ, [OIII], [NII] and [SII].
**Accuracy**: Measure throughput to 5%, wavelength position to about 5–10 pixels.
**Products**: ISR, new SYNPHOT tables.

## Cycle 8 Overview

In the previous section we described the Cycle 7 calibration plan. We expect the Cycle 8 calibration plan to largely mirror the Cycle 7 plan with two exceptions: we do not presently expect to continue either the PSF characterization program (7629) or the CTE characterization program (7630). We expect to obtain the necessary data for these programs in Cycle 7. We have recently added a Linear Ramp Filter (LRF) Calibration program to the Cycle 7 plan due to a recent discovery that errors in the LRF throughput may be as high as 8% rather than the 3% previously estimated. We do not expect that this program will be continued in Cycle 8, however. Similarly, we have no plans at present to include any further polarization calibration in Cycles 7 or 8; however, analysis of previous polarization calibration data is ongoing, and should any anomalies be found, we will adjust the calibration plans accordingly.

Table 1.4: WFPC2 Cycle 8 Calibration Plan

| ID | Proposal Title | Frequency | Estimated Time (orbits) | | Scheduling Required | Products | Accuracy Required | Notes |
|---|---|---|---|---|---|---|---|---|
| | | | "External" | "Internal" | | | | |
| **Routine Monitoring Programs** | | | | | | | | |
| 8441 8459 | WFPC2 Decons & Associated Observations | 1-2/4 weeks | 32 | 72 | every 28 days | Synphot, CDBS | 1-2% | Includes decons, photometric monitor, focus monitor, internals, UV throughput |
| 8442 | Standard Darks | weekly | | 324 | every 7 days | CDBS | 1 e/hr | Also hot pixel lists on WWW. |
| 8443 | Supplemental Darks (8460, 8461) | 0-3/day | | 1308 | anytime | | n/a | For archive only, no analysis provided |
| 8444 | Internal Monitor | 3/4 weeks | | 45 | every 7days | CDBS | 0.8e/pixel | New superbiases, not run on decon weeks |
| 8445 | Earth Flats | continuous | | 442 | mid-cycle | CDBS | 0.3% | Also LRF, Methane quads |
| 8446 | Astrometric Monitor | 2/cycle | 2 | | early & late | ISR | 0.05'' | Also K-spots & plate scale check in red |
| 8447 | CTE Monitor | 2/cycle | 4 | | mid- & late | ISR | 0.01 mag | |
| 8448 | Intflat and Visflat Sweeps | 1/cycle | | 43 | mid-cycle | TIR | 0.3% | Mostly intflats |
| 8449 | UV Flats Internal Monitor | 1/cycle | 2 | | mid-cycle | TIR | 2-8% | Uses UV cal channel lamp. |
| **Special Calibration Programs** | | | | | | | | |
| 8451 | Photometric Characterization | 1 | 2 | | mid-cycle | ISR | 2.5% | Subset of Cycle 7 proposal, as check. |
| 8452 | PSF Characterization | 1 | 2 | | late in cycle | CDBS | 10% | Subset of standard broadband filters. |
| 8453 | Polarization | 1 | 6 | 10 | early in cycle | CDBS | 3-5% | Subset of Cycle 6, as check |
| 8454 | Linear Ramp Filters | 1 | 4 | | late in cycle | CDBS | 3% | Placeholder, pending results from Cy.7. |
| 8450 | Noiseless Preflash | 1 | 5 | | early in cycle | TIR | 0.01 mag | Test scheme to reduce CTE problem |

Table 1.4: WFPC2 Cycle 8 Calibration Plan

| ID | Proposal Title | Frequency | Estimated Time (orbits) | | Scheduling Required | Products | Accuracy Required | Notes |
|---|---|---|---|---|---|---|---|---|
| | | | "External" | "Internal" | | | | |
| 8455 | Photometry of Very Red Stars | 1 | 2 | | mid-cycle | ISR | 2-5% | Outsourcing candidate. |
| 8456 | CTE for Extended Sources (2-3") | 1 | 4 | | mid-cycle | ISR | 0.01 mag | Outsourcing candidate. |
| 8457 | UV Earth Flats | continuous | | 720 | early in cycle | CDBS | 10% | Outsourcing candidate. |
| 8458 | Plate Scale Verification | 1 | 1 | | mid-cycle | ISR | 0.05% | Outsourcing candidate. |
| | ~10% reserve for unexpected items | | 7 | | | | | Placeholder. |
| TOTAL TIME (including all executions) | | | 73 | 2964 | | | | |

### Proposal IDs 8441, 8459: WFPC2 Cycle 8: Decontaminations and Associated Observations

**Purpose**: Monthly WFPC2 decons. Instrument monitors tied to decons: photometric stability check, focus monitor, pre- and post-decon internals--bias, intflats, K-spots, & darks, UV throughput checks.
**Description:** *Decontamination:* UV-blocking contaminants removed and hot pixels annealed, by warming the CCDs to +20C for 6 hours.
*Internals:* intflats, biases, darks & K-spots, before/after decons.
*Photometric and Focus Monitor:* Standard star GRW+70d5824 is observed after each decon and before every other decon: (1) F170W in all chips to monitor far UV contamination. (2) PC focus monitor observations in F439W, F555W, F814W. (3) F160BW, F218W, F255W, F336W, F439W, F555W, F814W observed in a different chip each month.
*UV Throughput:* PC & WF3 UV observations in all UV filters, popular UV filters in all chips, to verify that the UV spectral response curve is unchanged. Also check Methane quads.
**Products**: SYNPHOT, CDBS, Instrument Handbook, TIPS meetings, WWW reports, TIR, ISR.
**Accuracy**: *Photometry*: less than 2% discrepancy between results, 1% rms expected. *Focus measurement:* 1.5 micron accuracy, with a goal of 1 micron. *UV throughput:* better than 3%. *Flatfield:* temporal variations monitored at 1% level. *Gain ratios:* stable to better than 0.1%.

### Proposal ID 8442: WFPC2 Cycle 8: Standard Darks

**Purpose**: Measure dark current and identify of hot pixels.
**Description**: Six 1800s exposures/week with the shutter closed, five with clocks off, one with clocks on. This frequency is required due to the high formation rate of new hot pixels (several tens/CCD/day). Five darks per week are required for cosmic ray rejection, counterbalancing losses due to residual images, and improving the noise of individual measurements. Sometimes, no usable darks are available for a given week due to residual images, resulting in a longer-than-usual gap in the hot pixel lists. In a decon week, information on hot pixels that became hot and then annealed would be lost irretrievably. As a result, pre-decon darks (see Decon proposal) are executed in a non-interruptible sequence, at least 30 min after any WFPC2 activity.
**Products**: Weekly darks delivered to CDBS and monthly tables of hot pixels on the WWW. Superdark reference files.
**Accuracy**: Require ~1 $e^-$/hour (single-pixel rms) accuracy for most science applications. Expected accuracy in a typical superdark is 0.05 $e^-$/hour for normal pixels. The need for regular darks is driven by systematic effects, such as dark glow (a spatially and temporally variable component of dark signal) and hot pixels, which cause errors that may exceed these limits significantly.

### Proposal IDs 8443, 8460, 8461: WFPC2 Cycle 8: Supplemental Darks

**Purpose**: Obtain very frequent monitoring of hot pixels.
**Description**: This program is designed to provide up to three short (1000s) darks per day, to be used primarily for the identification of hot pixels. Shorter darks are used so that observations can fit into almost any occultation period, making automatic scheduling feasible. Supplemental darks will be taken at low priority, and only when there is no other requirement for that specific occultation period. This program is complementary with the higher priority Standard Darks proposal that has longer individual observations for producing high-quality pipeline darks and superdarks. Note that hot pixels are often a cause of concern for relatively short science programs, since they can mimic stars or mask key features of the observations. (About 400 new hot pixels/CCD are formed between executions of the Standard Darks program. These observations will be made available as a service to the GO community, and there is no plan to use them in our standard analysis and products.
**Products**: None.
**Accuracy**: n/a

### Proposal ID 8444: WFPC2 Cycle 8: Internal Monitor

**Purpose**: Verify the short-term instrument stability at both gain settings.
**Description**: Each set of internal observations consists of 8 biases (4 at each gain) and 4 INTFLATs (2 at each gain). The entire set should be run once per week, except for decon weeks, on a non-interference basis.
**Products**: Superbiases delivered annually to CDBS; TIPS reports on possible buildup of contaminants on the CCD windows (worms) as well as gain ratio stability, based on INTFLATs. A Technical Instrument Report will be issued if significant changes occur.
**Accuracy**: Approximately 120 bias frames are used for each superbias pipeline reference file, generated once a year; accuracy is required to be better than 1.5 e-/pixel, and is expected to be 0.8 e-/pixel.

### Proposal ID 8445: WFPC2 Cycle 8: Earth Flats

**Purpose**: Monitor flatfield stability.
**Description**: As in Cycle 7 programs 7625 & 8053, sets of 200 Earth-streak flats are taken to construct high quality narrow-band flatfields with the filters F375N, F502N, F656N and F953N. Of these 200 perhaps 50 will be at a suitable exposure level for destreaking. The resulting Earth superflats map the OTA illumination pattern and are combined with SLTV data (and calibration channel data in case of variation) for the WFPC2 filter set to generate a set of superflats capable of removing both the OTA illumination and pixel-to-pixel variations in the flatfields. The general plans of Cycles 5, 6, and 7 are repeated.
**Products**: New flatfields generated and delivered to CDBS if changes detected.

**Accuracy**: The single-pixel signal-to-noise ratio expected in the flatfield is 0.3%.

### Proposal ID 8446: WFPC2 Cycle 8: Astrometric Monitor

**Purpose**: Verify relative positions of WFPC2 chips with respect to one another.
**Description**: The rich field in ω Cen (same positions as Cycle 7 proposal 7627) is observed with large shifts (35’’) in F555W only, at two different times during Cycle 8. This will indicate whether there are shifts in the relative positions of the chips or changes in the astrometric solution at the sub-pixel level. Kelsall spot images will be taken in conjunction with each execution. The K-spots data and some external data indicate that shifts of up to 1 pixel may have occurred since mid-1994.
**Products**: TIPS, Technical Instrument Report, update of chip positions in PDB and of geometric solution in STSDAS tasks metric and wmosaic if significant changes are found.
**Accuracy**: relative positions determined to 0.05’’; variations to 0.01’’.

### Proposal ID 8447: WFPC2 Cycle 8: CTE Monitor

**Purpose**: Monitor CTE changes during Cycle 8.
**Description**: Observations of ω Cen (NGC 5139) are taken every 6 months during Cycle 8 to monitor changes in Charge Transfer Efficiency (CTE) of the WFPC2 (extension of Cycle 7 proposal 7929). The principal observations will be in F814W at gain 15 in WF2 and WF4. Supplemental observations at gain 7, in WF3, and with a preflash will be performed if time permits, along with observations in F439W and F555W. For each visit, observations will be done in single guide star mode.
**Products**: Instrument Science Report
**Accuracy**: 0.01 magnitudes.

### Proposal ID 8448: WFPC2 Cycle 8: Intflat and Visflat Sweeps

**Purpose**: Monitor the pixel-to-pixel flatfield response and the VISFLAT lamp degradation, as well as detect any possible changes due to contamination. The linearity test obtains a series of INTFLATs with both gains and both shutters. Since the INTFLATs have significant spatial structure, any nonlinearity would appear as a non-uniform ratio of INTFLATs with different exposure times.
**Description**: *VISFLAT mini-sweep:* pre- and post-decon observations using the photometric filter set at gain 7, and FR533N at both gains to test the camera linearity. *INTFLAT sweep:* taken within a two-week period. Almost all filters used, some with both blades and gains, others with just one blade and gain. *Linearity test:* done at both gains and blades using F555W, and an additional set with one blade and gain with clocks=on.
**Products**: TIPS, TIR if any significant variations are observed.
**Accuracy**: *VISFLATs:* stable to better than 1% in overall level and spatial variations (after correcting for lamp degradation). Contamination effects

should be < 1%. *INTFLATs:* signal-to-noise ratio per pixel similar to the VISFLATs, but spatial and wavelength variations in the illumination pattern are much larger. (INTFLATs will provide a baseline comparison of INTFLAT vs. VISFLAT if the CAL channel system fails.)

### Proposal ID 8449: WFPC2 Cycle 8: UV Flats Internal Monitor

**Purpose**: Monitor the stability of UV flatfield.
**Description**: UV flatfields obtained with the CAL channel's ultraviolet lamp (UVFLAT) using the UV filters F122M, F170W, F160BW, F185W, & F336W. The UV flats are used to monitor UV flatfield stability and the stability of the F160BW filter by using F170W as the control. The F336W ratio of VISFLAT to UVFLAT provides a diagnostic of the UV flatfield degradation & ties the UVFLAT and VISFLAT flatfield patterns. Two supplemental dark frames must be obtained immediately after each use of the lamp to check for possible after-images.
**Products**: New UV flatfields if changes are detected.
**Accuracy**: About 2-8% pixel-to-pixel expected (depending on filter).

### Proposal ID 8451: WFPC2 Cycle 8: Photometric Characterization

**Purpose**: Determine whether any changes in the zeropoint, the spatial dependence of the zeropoint, or contamination rates have occurred, by comparing with the baseline measurements for GRW+70D5824 (single photometric standard with 13 filters)
**Description**: Observe the standard star GRW+70D5824 in PC1 and WF3 using filters F380W, F410M, F450W, F467M, F547M, F569W, F606W, F622W, F702W, F785LP, F791W, F850LP, and F1042M. Observations should be done within 7 days after a decon. These observations will be compared with data from the Cycle 7 program 7628.
**Products**: TIR, SYNPHOT update if necessary.
**Accuracy**: 2% photometry.

### Proposal ID 8452: WFPC2 Cycle 8: PSF Characterization

**Purpose**: Provide a check of the subsampled PSF over the full field.
**Description**: Observations using only two of the standard broadband filters (F555W and F814W). With one orbit per photometric filter, DITHER-LINE and POS TARG observations are performed in a 4x4 parallelogram. The dither-line-spacing=0.177, and POS TARG steps are 0.125; this gives a critically sampled PSF over most of the visible range. Each star is measured 16 times per filter at different pixel phase, providing a high S/N, critically sampled PSF. This will improve the quality of PSF fitting photometry.
**Products**: PSF library (WWW). Updates for TIM and TINYTIM. Accurate empirical PSFs to be derived for PSF fitting photometry.
**Accuracy**: Results will be limited by breathing variations in focus, so predicting PSF accuracy is difficult. (For breathing < 5 micron

peak-to-peak, PSFs should be good to ~10% in each pixel.) Proposal provides a measurement of pixel phase effect on photometry (sub-pixel QE variations exist), and gives a direct measurement of sub-pixel phase effects on photometry, measured to better than 1%.

### Proposal ID 8453: WFPC2 Cycle 8: Polarization

**Purpose**: Verify stability of polarization calibration.
**Description**: The data from this proposal will be used to identify any changes that may have occurred since the polarizer calibration in Cycle 5. Two stars will be observed, G191B2B and BD+64D106, a non-polarized and polarized standard star, respectively. The unpolarized star will be observed in 2 visits with the ORIENT changed by 90 degrees between visits, so as to sample any residual polarization of the star. The polarized star will be observed in 4 visits with the ORIENT changed by 45 degrees between visits, so as to fully sample the properties of each polarizer quad. Each visit consists of F555W exposures in PC1 and WF3, followed by F555W+POLQ exposures in PC1, WF2, WF3, and WF4. Other popular broadband filters (F300W, F439W, F675W, and F814W) will be checked using only the unrotated polarizer. Finally, a small set of VISFLATs (with a minimum of lamp cycles) will be included to check for flatfield changes.
**Products**: TIR or ISR report. If necessary, update SYNPHOT tables, WWW polarization calibration tools, and CDBS flatfields.
**Accuracy**: Expected accuracy is <3%.

### Proposal ID 8454: WFPC2 Cycle 8: Linear Ramp Filter

**Purpose**: Check wavelength and throughput calibration for LRFs at selected wavelengths.
**Description**: A thorough check of the linear ramp filters (LRFs) is being done as part of the Cycle 7 calibration program, where the UV spectrophotometric standard (GRW+70d5824) is observed at 75 different wavelengths and an extended source (Orion nebula) is observed for an orbit as well. This proposal is currently a placeholder, pending data analysis results from the Cycle 7 program. We anticipate requiring 4 orbits to spot-check some of the more popular wavelengths as well as cover any wavelengths requested by Cycle 8 GOs that weren't observed as part of the Cycle 7 calibration program.
**Products**: Updates to SYNPHOT tables if necessary and an ISR.
**Accuracy**: Throughput accuracy should be better than 3%.

### Proposal ID 8450: WFPC2 Cycle 8: Noiseless Preflash

**Purpose**: Test effectiveness of "Noiseless" preflash in reducing CTE and long vs. short Photometric effects.
**Description**: A globular cluster is observed both before and after a preflash that has been read out (i.e. noiseless). The preflash will be tailored to expose the CCDs to about 3000 DN without saturation. The hypothesis is that the traps in the CCD will remain filled even though the preflash has

been read out, thereby minimizing the effects of CTE. The observation sequence is repeated at two detector positions and exposure times, so as to test for CTE and long vs. short effects. The four orbits are done in one non-interruptible visit, which is preceded by a pair of 1800s darks and includes single darks during occultation periods, to insure that no prior exposures will effectively preflash the non-preflash exposures.
**Products**: Improved observing strategies; ISR.
**Accuracy**: 1% photometry

### Proposal ID 8455: WFPC2 Cycle 8: Photometry of Very Red Stars

**Purpose**: Verify the photometric calibration of WFPC2 filters and obtain estimated color terms (HST to Johnson) for late M stars.
**Description**: WFPC2 imaging (F439W, F555W, F675W, F814W) of two well-known M dwarfs, VB8 and VB10, for which ground-based measurements in the Johnson filters exist. Use two different y positions to account for CTE. The current calibration is based on white dwarf and solar analog data, which are insufficient to produce an accurate calibration for cool red stars (late K and M) in broad-band filters. The calibration of cool stars is especially difficult at the red end (F814W), because their spectra can rise quickly where the DQE drops substantially (increasing the uncertainty in the synthetic magnitude calibration). The observations of two well-studied late M stars, VB8 and VB10, will provide a direct empirical calibration of these effects and reduce the uncertainties in the photometric response of WFPC2 for very red stars.
**Products**: N/A
**Accuracy**: Better than 0.03 mag.

### Proposal ID 8456: WFPC2 Cycle 8: CTE for Extended Sources

**Purpose**: Determine the effect of Charge Transfer Efficiency (CTE) on small extended sources.
**Description**: Previous CTE proposals have all focused on stellar targets. This proposal is aimed at observing small (~2-3”) extended sources in a suitable galaxy cluster. The target (tentatively cluster 135951+621305, at z=0.3) will be observed in WF2 and WF4, in F606W and F814W. The filter F606W is chosen instead of the F555W used for stellar CTE measurements, to allow a comparison to archival images for estimating of any possible time-dependence. One orbit is needed for each pointing for each filter, for a total of four orbits.
**Products**: ISR
**Accuracy:** 10%

### Proposal ID 8457: WFPC2 Cycle 8: UV Earth Flats

**Purpose**: Improve quality of pipeline UV flatfields.

**Description**: Earth streak-flats are taken in UV filters (F170W, F185W, F218W, F255W, F300W, F336W, and F343N). Those UV filters with significant redleak will also be observed crossed with selected broadband filters (F450W, F606W, F675W, and F814W), in order to assess and remove the redleak contribution. Earth Flats required: 100 for each of the 7 UV filters plus 20 with each of the crossed filter sets (16 combinations).
**Products**: Updated flatfields for pipeline via CDBS.
**Accuracy**: 10%

### Proposal ID 8458: WFPC2 Cycle 8: Plate Scale Verification

**Purpose**: Check of the WFPC2 plate scale in the UV and red.
**Description**: UV and F953N observations of the bright cluster NGC2100. Data will be taken in F170W, F218W, F300W, F555W (to allow tie-in to previous observations) and F953N. To minimize orbits required, the program is designed around short exposures in the filters listed above; the data will provide a verification the plate scale in the UV but exposure times will not be long enough to allow a full distortion solution.
**Products**: ISR
**Accuracy**: Better than 0.05% (0.4 pixels over 1 chip), or 0.05 mas/pixel in WF.

# References


- Baggett, S., et al, 1998, WFPC2 TIR 98-03 “WFPC2 Dark Current Evolution”
- Baggett, S., Gonzaga, S., 1998, WFPC2 ISR 98-03 “WFPC2 Long-Term Photometric Stability”
- Biretta, J., Baggett, S., 1998, WFPC2 TIR 98-04: “Proposed Modification to the WFPC2 SAA Avoidance Contour” (plus update)
- Biretta, J., McMaster, M., 1997, WFPC2 ISR 97-11 “WFPC2 Polarization Calibration”
- Biretta, J., Mutchler, M., 1998, WFPC2 ISR 97-05 “Charge Trapping and CTE Residual Images in the WFPC2 CCDs”
- Casertano, S., 1998, WFPC2 ISR 98-02 “The Long vs. Short Anomaly in WFPC2 Images”
- Casertano, S., et al., editors, *The 1997 HST Calibration Workshop Proceedings*, STScI, 1998.[4]


4. Available at

http://www.stsci.edu/stsci/meetings/cal97/proceedings.html

- Fruchter, A. S., Hook, R. N., 1997, "A novel image reconstruction method applied to deep Hubble Space Telescope images," in *Applications of Digital Image Processing XX*, Proc. SPIE, Vol. 3164, A. Tescher, editor, p.120.
- Gonzaga, S., et al, 1998, WFPC2 ISR 98-04 "The Drizzling Cookbook"
- Gonzaga, S., et al, 1999, WFPC2 TIR 99-01 "WFPC2 Aperture Photometry Corrections as a Function of Chip Position"
- Holtzman, J., et al, 1995a, "The Performance and Calibration of WFPC2 on the Hubble Space Telescope," *PASP*, 107, 156.
- Holtzman, J., et al, 1995b, "The Photometric Performance and Calibration of WFPC," *PASP*, 107, 1065.
- Suchkov, A., Casertano, S., 1997, WFPC2 ISR 97-01 "Impact of Focus Drift on Aperture Photometry"
- Voit, M., ed., *HST Data Handbook*, (Version 3.0, October 1997).[5]
- Whitmore, B., 1998, "Time Dependence of the Charge Transfer Efficiency on the WFPC2."[6]
- Whitmore, B., Heyer, I., 1997, WFPC2 ISR 97-08 "New Results on Charge Transfer Efficiency and Constraints on Flat-Field Accuracy." (updated in 1998)


# New WFPC2 Documentation, 1997-1999

## Instrument Science Reports

Available online at

http://www.stsci.edu/instruments/wfpc2/wfpc2_bib.html.

- 99-01: Internal Flat Field Monitoring II. Stability of the Lamps, Flat Fields, and Gain Ratios (not on the web yet) - O'Dea, Mutchler, Wiggs.
- 98-04: The Drizzling Cookbook - Gonzaga et al.

5. Available at:

http://www.stsci.edu/documents/data-handbook.html.

6. Available at:

http://www.stsci.edu/instruments/wfpc2/Wfpc2_isr/cte_vs_time_post.ps

- 98-03: WFPC2 Long-Term Photometric Stability - Baggett and Gonzaga.
- 98-02: The Long vs. Short Anomaly in WFPC2 Images - Casertano and Mutchler.
- 98-01: WFPC2 Cycle 6 Calibration Closure Report - Baggett, et al.
- 97-11: WFPC2 Polarization Calibration - Biretta and McMaster.
- 97-10: WFPC2 SYNPHOT Update - Baggett, et al.
- 97-09: Results of the WFPC2 Post-Servicing Mission-2 Calibration Program - Biretta, et al.
- 97-08: New Results on Charge Transfer Efficiency and Constraints on Flat-Field Accuracy - Whitmore and Heyer.
- 97-07: WFPC2 Electronics Verification - Stiavelli and Mutchler.
- 97-06: WFPC2 Cycle 7 Calibration Plan - Casertano, et al.
- 97-05: Charge Trapping and CTE Residual Images in the WFPC2 CCDs - Biretta and Mutchler.
- 97-04: Properties of WFPC2 Bias Frames - O'Dea, et al.
- 97-03: Summary of WFPC2 SM97 Plans - Biretta, et al.
- 97-02: WFPC2 Cycle 5 Calibration Closure Report - Casertano and Baggett.
- 97-01: Impact of Focus Drift on Aperture Photometry - Suchkov and Casertano.

## Technical Instrument Reports

Internal memos, available by request to `help@stsci.edu`.

- TIR WFPC2 99-01: WFPC2 Aperture Photometry Corrections as a Function of Chip Position.
- TIR WFPC2 98-04: Addendum to TIR 98-04.
- TIR WFPC2 98-04: Proposed Modification to the WFPC2 SAA Avoidance Contour.
- TIR WFPC2 98-03: WFPC2 Dark Current Evolution.
- TIR WFPC2 98-02: Analysis of the Excess Charge in WFPC2 Over-scans.
- TIR WFPC2 98-01: Time Dependence of the CTE on the WFPC2.
- TIR WFPC2 97-11: Long-Term Study of Bias Jumps.

- TIR WFPC2 97-10: WFPC2 Photometry from Subtraction of Observed PSFs.
- TIR WFPC2 97-09: The WFPC2 PSF Library.
- TIR WFPC2 97-08: SMOV Flat Field Check.
- TIR WFPC2 97-07: WFPC2 Internal Monitoring for SM97.
- TIR WFPC2 97-06: SMOV Check of WFPC2 PSF Stability.
- TIR WFPC2 97-05: Results of the WFPC2 SM-2 Lyman-Alpha Throughput Check.
- TIR WFPC2 97-04: VISFLAT Channel Monitoring.
- TIR WFPC2 97-03: OTA Focus during SMOV.
- TIR WFPC2 97-02: SM-2 UV Monitoring and Cooldown Procedure.
- TIR WFPC2 97-01: Results of the WFPC2 SMOV Relative Photometry Check.

## Other Selected Documents

Available online at:

http://www.stsci.edu/instruments/wfpc2/wfpc2_doc.html.

- The WFPC2 Instrument Handbook, Version 4.0
- The HST Data Handbook, Version 2.0
- The WFPC2 Tutorial, a step-by-step guide to reducing WFPC2 data
- STAN, The Space Telescope Analysis Newsletter
- The WFPC2 History memo, containing chronological information on decontaminations, darks, focus changes, and miscellaneous items
- How to calibrate WFPC2 Linear Ramp Filter data
- Time Dependence of the Charge Transfer Efficiency
- The WFPC2 Reference Files, a complete list of all reference files available for recalibrating WFPC2 data
- The STSDAS SYNPHOT User's Guide
- The Guide to WFPC2 SYNPHOT Tables, which describes the use of the STSDAS task SYNPHOT for WFPC2 photometry
- WFPC2 Photometry and SYNPHOT
- Table of up-to-date SYNPHOT photflams and zeropoints

# Index